

THESIS ON NATURAL AND EXACT SCIENCES B69

**Chemical Spray Pyrolysis Deposition of Zinc Sulfide  
Thin Films and Zinc Oxide Nanostructured Layers**

TATJANA DEDOVA

TALLINN 2007

TALLINN UNIVERSITY OF TECHNOLOGY  
Faculty of Chemistry and Materials Technology  
Department of Materials Science  
Chair of Semiconductor Materials Technology

**Dissertation was accepted for the defence of the degree of Doctor of Philosophy in Chemistry and Materials Technology on October 05, 2007**

**Supervisor:** Research Professor Malle Krunks, Department of Materials Science

**Opponents:** Professor Lauri Niinistö, Helsinki University of Technology, Helsinki, Finland  
Dr. Thierry Pauporté, Laboratoire d'Électrochimie et de Chimie Analytique, École Nationale Supérieure de Chimie de Paris, France

**Defence of the thesis:** December 7, 2007, at 13.30,  
Lecture hall: VII-131,  
Tallinn University of Technology, Ehitajate tee 5, Tallinn

**Declaration:** Hereby I declare that this doctoral thesis, my original investigation and achievement, submitted for the doctoral degree at Tallinn University of Technology has not been submitted for any academic degree.

Tatjana Dedova

Copyright: Tatjana Dedova 2007

ISSN 1406-4723

ISBN 978-9985-59-743-9

LOODUS-JA TÄPPISTEADUSED B69

**Tsinksulfiidi õhukesed kiled ning tsinkoksiidi  
nanostruktuursed kihid keemilise pihustuspürolüüsi  
meetodil**

TATJANA DEDOVA

TALLINN 2007

## Table of contents

|   |    |
|---|----|
| LIST OF PUBLICATIONS .....  | 6  |
| AUTHOR'S OWN CONTRIBUTION.....  | 7  |
| LIST OF ABBREVIATIONS .....   | 8  |
| INTRODUCTION .....  | 9  |
| 1. LITERATURE OVERVIEW AND AIM OF THE STUDY .....                                   | 11 |
| 1.1 Chemical spray pyrolysis (CSP).....   | 11 |
| 1.1.1 Introduction to the CSP .....   | 11 |
| 1.1.2 Description of the CSP .....  | 11 |
| 1.1.3 Advantages and disadvantages of the CSP .....                                 | 13 |
| 1.2 ZnS thin films .....  | 13 |
| 1.2.1 Introduction to the thin film technology.....                                 | 13 |
| 1.2.2 Material properties of ZnS .....  | 13 |
| 1.2.3 Application of ZnS thin films .....   | 14 |
| 1.2.4 Deposition methods for ZnS thin films .....                                   | 15 |
| 1.2.5 ZnS thin films by CSP .....   | 15 |
| 1.3 ZnO nanostructures .....  | 17 |
| 1.3.1 Introduction to the nanostructures.....                                       | 17 |
| 1.3.2 Material properties of ZnO .....  | 17 |
| 1.3.3 Applications of ZnO nanostructures.....                                       | 19 |
| 1.3.4 ZnO films deposition by CSP .....   | 20 |
| 1.3.4 Synthesis methods for ZnO nanostructures .....                                | 21 |
| 1.3.5 Growth mechanisms of ZnO nanorods and nanowires.....                          | 25 |
| 1.4 Summary of the literature review and aim of the study .....                     | 26 |
| 2. EXPERIMENTAL.....  | 28 |
| 2.1 Spray pyrolysis deposition procedure .....                                      | 28 |
| 2.1.1 Preparation of ZnS thin films.....  | 28 |
| 2.1.2 Preparation of ZnO nanostructured layers .....                                | 28 |
| 2.2 Characterisation methods for ZnS thin films and ZnO nanostructured layers ..... | 28 |
| 3. RESULTS AND DISCUSSION.....  | 30 |
| 3.1 Deposition of ZnS thin films by CSP.....  | 30 |
| 3.1.1 Structure, phase and elemental composition of sprayed ZnS thin films.....     | 30 |
| 3.1.2 Morphology of sprayed ZnS thin films .....                                    | 34 |
| 3.1.3 Optical properties of sprayed ZnS films.....                                  | 34 |
| 3.1.4 Conclusions on ZnS thin films.....  | 37 |
| 3.2 Deposition of ZnO nanostructured layers by CSP.....                             | 37 |
| 3.2.1 Effect of the deposition temperature .....                                    | 38 |
| 3.2.2 Effect of the precursor concentration .....                                   | 40 |

|   |    |
|---|----|
| 3.2.3 Effect of the substrates .....                  | 42 |
| 3.2.4 Effect of solvent and additive .....            | 44 |
| 3.2.5 Properties of spray-deposited ZnO nanorods..... | 49 |
| CONCLUSIONS .....                                     | 52 |
| ACKNOWLEDGEMENTS .....                                | 54 |
| ABSTRACT .....  | 55 |
| KOKKUVÕTE .....                                       | 57 |
| REFERENCES .....                                      | 59 |
| Appendix A .....                                      | 69 |
| Appendix B .....                                      | 76 |

## LIST OF PUBLICATIONS

The thesis is based on the following publications, which are referred to in the text by the Roman numerals **I-VII**:

- I **T. Dedova**, M. Krunk, O. Volobujeva and I. Oja. ZnS thin films deposited by spray pyrolysis technique. - *Physica Status Solidi c*, 2005, 3, p.1161-1166.
- II **T. Dedova**, A. Mere, O. Kijatkina, I. Oja, O. Volobujeva and M. Krunk. Structural and optical characterization of sprayed ZnS thin films. - *Proceedings of SPIE 5946: 2005*, p.34-40.
- III M. Krunk, **T. Dedova** and I. Oja. Spray pyrolysis deposition of nanostructured Zinc Oxide thin films. - *Thin Solid Films*, 2006, 515, p. 1157-1160.
- IV **T. Dedova**, M. Krunk, M. Grossberg, O. Volobujeva and I. Oja Acik. A novel deposition method to grow ZnO nanorods: spray pyrolysis. - *Superlattices and Microstructures*, 2007, 42, p. 444-450.
- V **T. Dedova**, M. Krunk, A. Mere, J. Klauson and O. Volobujeva. Preparation of shape and size-controlled zinc oxide nanostructures by chemical spray pyrolysis technique. *Materials Research Society Symposium Proceedings 957: Warrendale, PA, 2007*, p. 0957-K10-26.
- VI **T. Dedova**, O. Volobujeva, J. Klauson, A. Mere and M. Krunk. ZnO nanorods via spray deposition of solutions containing zinc chloride and thiocarbamide. - *Nanoscale Research Letters, Nanoexpress*, 2007, 2, p.391-396.
- VII M. Krunk, I. Oja and **T. Dedova**. Method of preparing zinc oxide nanorods on a substrate by chemical spray pyrolysis, international patent application WO2006/108425 (Priority No. US20050671232P, priority date 04/14/2005).

In the appendix A, copies of these publications are included.

## **AUTHOR'S OWN CONTRIBUTION**

The contribution by the author to the papers included in the thesis is as follows:

- I** ZnS thin films deposition, films characterization (FTIR absorbance spectra measurements in the MIR region), analysis of the results, minor role in writing
- II** ZnS thin films deposition and characterization (UV-VIS measurements, band gap calculations, FTIR measurements, refractive index calculations using the fringe method), analysis of the results, major role in writing.
- III** ZnO layers deposition and characterization (UV-VIS measurements), analysis of the results, minor role in writing
- IV** ZnO layers deposition, analysis of the results, minor role in writing
- V** ZnO layers deposition, analysis of the results, major role in writing
- VI** ZnO layers deposition, analysis of the results, major role in writing
- VII** ZnO layers deposition

## LIST OF ABBREVIATIONS

|        |   |
|--------|---|
| ALD    | Atomic Layer Deposition                           |
| AOO    | Anodized Aluminum Oxide                           |
| CBD    | Chemical Bath Deposition                          |
| CSP    | Chemical Spray Pyrolysis                          |
| CVD    | Chemical Vapor Deposition                         |
| DEZ    | Diethyl Zinc                                      |
| DSSC   | Dye-Sensitized Solar Cell                         |
| EDX    | Energy Dispersive X-ray Analysis                  |
| $E_g$  | Band gap  |
| ED     | Electrodeposition                                 |
| ESB    | Energy and Selected Back-scattered electron image |
| ETA    | Extremely Thin Absorber                           |
| FTIR   | Fourier Transform Infrared Spectroscopy           |
| FWHM   | Full Width at Half Maximum                        |
| IR     | Infrared  |
| ITO    | Indium Tin Oxide                                  |
| JCPDS  | Joint Committee on Powder Diffraction Standards   |
| L/d    | Aspect ratio (Length/diameter) of the crystal     |
| LED    | Light Emitting Diode                              |
| MOCVD  | Metal Organic Chemical Vapor Deposition           |
| MIR    | Middle Infrared                                   |
| NBE    | Near Band Edge                                    |
| NIR    | Near Infrared                                     |
| PL     | Photoluminescence                                 |
| PECVD  | Plasma Enhanced Chemical Vapor Deposition         |
| PVD    | Physical Vapor Deposition                         |
| RF     | Radio-Frequency (Sputtering)                      |
| SA     | Self Activated                                    |
| SAED   | Selected Area Electron Diffraction                |
| SEM    | Scanning Electron Microscopy                      |
| SILAR  | Successive Ionic Layer Adsorption and Reaction    |
| SPIE   | Society of Photographic Instrumentation Engineers |
| TEM    | Transmission Electron Microscopy                  |
| TCO    | Transparent Conductive Oxide                      |
| tu     | thiocarbamide, thiourea                           |
| UV-VIS | Ultraviolet-Visible (Spectroscopy)                |
| VS     | Vapor Solid                                       |
| VLS    | Vapor-Liquid-Solid                                |
| XRD    | X-ray Diffraction                                 |



## INTRODUCTION

The synthesis of low dimensional materials comprising thin films and nanostructures from easily available and environmentally friendly starting materials along with exploration of cost-effective deposition methods are main challenges of today's materials science.

Addressing to these issues, this thesis is devoted to the systematic study on the fabrication and characterization of ZnS thin films and ZnO nanostructured layers by chemical spray pyrolysis (CSP). A highly important issue for the practical application of materials is controlled and reproducible growth.

Chemical spray pyrolysis (CSP) is commercially attractive method for the production of high quality, uniform and well-crystalline compounds in a short time at low cost [1, 2, 3].

ZnS thin films are very important semiconductor material with wide range of applications, such as electroluminescent displays [4], light emitting diodes [1, 5], optical sensors [6] and solar cells [7].

Up to the beginning of the present investigation a very limited number of studies was reported on sprayed ZnS thin films. ZnS thin films were deposited only at fixed molar ratio of the precursors ( $\text{ZnCl}_2$  and thiourea) as 1:1 [1, 8, 9]. However, it has been demonstrated earlier that  $\text{ZnCl}_2$  and thiourea form the dichlorobis(thiourea)zinc complex in an aqueous solution (Zn:S in the complex is 1:2) and ZnS is formed upon thermal decomposition of this complex compound [10-12]. Strong effect of molar ratio of the precursors in solution on properties of sprayed CdS thin films have also been demonstrated earlier [13, 14-17]. However, the influence of molar ratio of initial components ( $\text{ZnCl}_2$  and thiocarbamide) on structural, optical, morphological properties of ZnS thin films has not been sufficiently studied. This thesis comprises an extended study on the effect of molar ratio of the precursors at various deposition temperatures on the structure, morphology, composition and optical properties of sprayed ZnS thin films. Obtained results are published in papers I, II and summarized in chapter 3.1 of the thesis.

The second part of the thesis is devoted to a pioneering work on synthesis and characterization of ZnO nanostructured layers comprising nanorods by CSP. Due to high surface area and small dimensions ZnO nanorod arrays demonstrate unique mechanical, optical, electronic, and magnetic properties [18-20]. These structures are very attractive for possible applications in new generation nanodevices such as light emitting diodes, solar cells, sensors etc [21, 22]. Thus, the cost-effective fabrication of ZnO nanorod arrays along with controlled growth of certain size, shape, properties and orientation is highly important.

The studies on ZnO nanorod formation, morphology, structure and crystalline properties as a function of the growth temperature, precursor solution composition and concentration, and type of substrate are reported in papers III-VI and

summarized in chapter 3.2 of the thesis. Newly invented method of ZnO nanorods preparation is protected by the international patent application [VII].

The work is financially supported by the Estonian Science Foundation grants ETF5612 and ETF6954, EU FP5 project ENK6-CT-2002-80664 and Estonian Doctoral School of Materials Science and Materials Technology (MMTDK).

# **1. LITERATURE OVERVIEW AND AIM OF THE STUDY**

## **1.1 Chemical spray pyrolysis (CSP)**

In this study chemical spray pyrolysis deposition method has been chosen for preparation of ZnS thin films and ZnO nanostructured layers. The description of this method, along its advantages and disadvantages are presented in this chapter.

### **1.1.1 Introduction to the CSP**

CSP technique has been developed in 1966 by Chamberlin and Skarman [13] for the deposition of CdS and CdSe films. Nowadays it is widely used to synthesize a variety of metal oxides as well as binary and ternary chalcogenides in different forms like dense or porous thin films and powders [23]. Materials obtained by CSP find a wide range of applications in solar cells, optoelectronic devices, antireflective coatings, sensors, etc. [2, 24].

### **1.1.2 Description of the CSP**

Chemical spray pyrolysis is a process where a precursor solution, containing the constituent elements of the compound, is pulverised in the form of tiny droplets onto the preheated substrate, where upon the thermal decomposition of the precursor an adherent film of thermally more stable compound forms [14] Figure 1.1 shows the schematic representation of a CSP set-up which is generally used [13] and also employed in this work for the growth of the ZnS thin films and ZnO nanostructured layers [I–VII]. CSP set-up consists of 1) an atomizer, 2) precursor solution, 3) substrate heater, 4) temperature controller, 5) air compressor or other source of carrier gas, 6) rotameter.

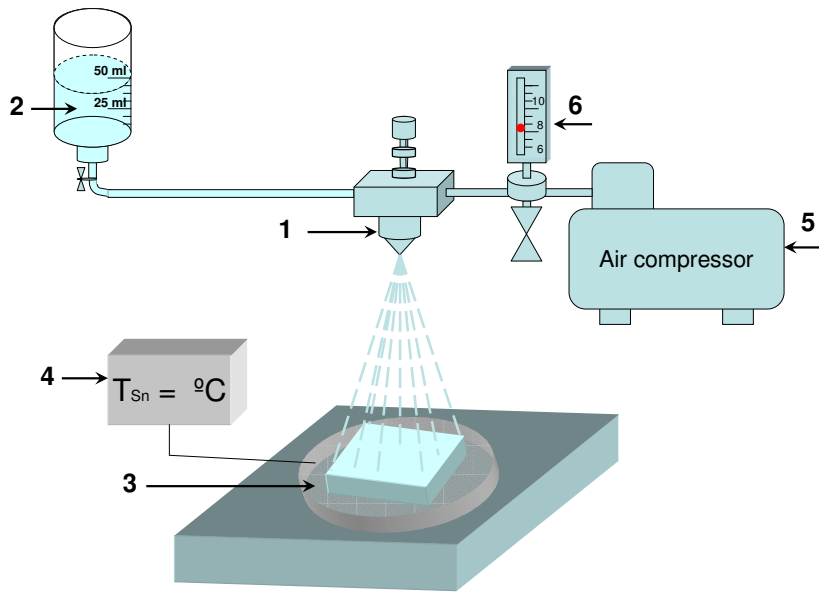


**Figure 1.1 Set-up of the chemical spray pyrolysis system used in this work**

In practice, spray pyrolysis involves several stages: 1) generation micro-sized droplets of precursor solution, 2) evaporation of solvent, 3) condensation of solute, 4) decomposition of the precursor or solute and 5) sintering of the solid particles. It is highly important that precursor should not volatilize before decomposition [25]. The substrate temperature is the key parameter in spray pyrolysis process that determines the final compound morphology and properties. By increasing the temperature, the morphology of the final product can change from well adherent thin film to a cracked layer, or to a porous film or structured layer. Other important parameters which influence the deposition process and thus the final product quality are: nature of the substrate, the solution composition and properties of its components (volatility, viscosity, chemical stability etc.), the gas and solution flow rates, deposition time, solution amount and the nozzle to the substrate distance [26]. The nature of the substrate controls the nucleation and crystal growth which can have a significant influence on the properties of the final material. For instance, in this work it was demonstrated that the formation of ZnO nanorods by spray was drastically affected by the nature of the substrate [III–V]. Very volatile solvents may lead to cracking layers as the film dries up before the precursor is pyrolyzed [27].

The sprayed layer thickness depends upon the concentration of the precursor solution and the quantity of the precursor solution sprayed, substrate temperature, distance between the spray nozzle and substrate, etc. In addition, the final product

properties and morphology can be easily modified by using various additives in the precursor solution.

### **1.1.3 Advantages and disadvantages of the CSP**

In general, CSP is a convenient, simple and low-cost method for the deposition of large-area thin films, and it has been used for a long time. In addition to its simplicity, CSP has a number of other advantages: 1) Low cost (inexpensive apparatus, does not require high quality targets or vacuum); 2) Easy control of composition and microstructure (facile way to dope material by merely adding doping element to the spray solution); 3) deposition at moderate temperatures of 100–500 °C; 4) Technological ability for mass production [2, 24, 26].

However as every other method, CSP has some disadvantages, main ones of them can be listed as follows: 1) possible oxidation of sulfides when processed in air atmosphere; 2) difficulties with growth temperature determination; 3) after long processing time spray nozzle may become cluttered; 4) films quality may depend on the droplet size and spray nozzle.

Anyway, the value of CSP advantages makes this method attractive and competitive compared to many other techniques used for materials synthesis.

## **1.2 ZnS thin films**

This part of the thesis gives a short introduction to thin film technology, an overview on ZnS properties, ZnS thin films applications and preparation techniques with emphasis on the studies done on ZnS thin films by spray pyrolysis.

### **1.2.1 Introduction to the thin film technology**

A **thin film** is defined as a low-dimensional material created by condensing, one-by-one, atomic/molecular/ionic species of matter. The thickness is typically less than several microns [28]. Thin film technology is pervasive in many applications, including microelectronics, optics, magnetic, hard and corrosion resistant coatings, micro-mechanics, etc [29].

### **1.2.2 Material properties of ZnS**

Zinc sulfide is highly important semiconductor material which belongs to the group of II–VI wide band gap semiconductors. ZnS exists in two crystallographic forms having cubic (sphalerite or zincblende) or hexagonal (wurtzite) crystal structure (Figure 1.2 a and b, respectively). It has been established earlier that sphalerite to wurtzite transition occurs at temperatures of 1020 °C at atmospheric pressure [30, 31]. However there are some reports stating the sphalerite to wurtzite transition temperature as a function of both growth temperature and sulfur fugacity. High sulfur fugacity leads to the zinc vacancies and transition temperatures about 1000°C. Sulfur vacancies, resulting from low sulfur fugacities, can decrease the

transition temperature below 500 °C [32]. For instance, ZnS films with hexagonal structure were prepared at 425–500 °C by ALD [33, 34] and at 400 °C by physical vapor deposition (PVD) [35].

ZnS has a direct transition type band structure. The cubic form has a band gap of 3.54–3.6 eV, whereas the band gap of hexagonal form is higher being 3.74–3.87 eV [46–38]. ZnS exhibits high transparency over the wide spectrum region between 380 nm and 25 μm. The refractive index ( $n$ ) of bulk ZnS is 2.47 at 450.9 nm and 2.32 at 708.5 nm, with the corresponding extinction coefficient ( $k$ ) varying in the  $10^{-5}$  to  $10^{-6}$  range [5]. The electrical resistivity is in the order of  $10^4$  Ωcm with n-type electrical conductivity. It can be doped as both n- and p-type semiconductor, which is unusual for the II–VI semiconductors. Zinc sulfide may be activated for photo-, electro- and cathode-luminescent emission by a variety of elements including: Mn, Cu, Ag, Au, P, As, Sb, Pb, V, Fe, Na, Li, Ga, In, etc. [29].

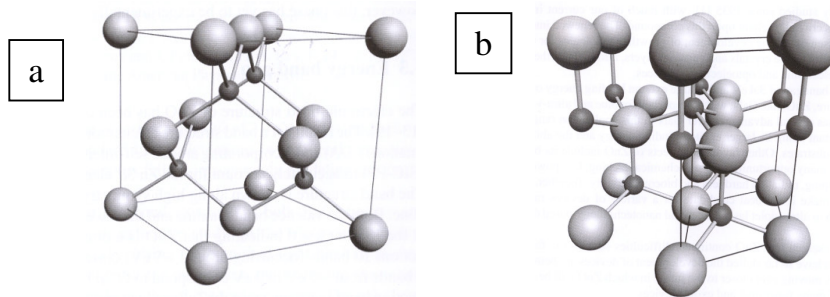


**Figure 1.2 a) The zinc blende b) wurtzite crystal structures of ZnS, S atoms are shown as white large spheres, Zn atoms are small black spheres [39]**

### 1.2.3 Application of ZnS thin films

ZnS thin films are one of the most important semiconducting materials having superior intrinsic properties and a wide range of applications in optoelectronic devices [1, 5, 40, 41].

Zinc sulfide is considered important for applications in ultraviolet–light–emitting diodes (LEDs), flat–panel displays (Mn–doped electroluminescent panels, Ag–, Cu–, Al– or In–doped cathodoluminescent panels), infrared windows, sensors and lasers. A diverse range of solar device applications exists for ZnS thin films, including filters, anti–reflection coatings in silicon based solar cells and heterojunction part (buffer layer) of the chalcopyrite semiconductor–based solar cells [42]. The higher bandgap of ZnS (3.6–3.8 eV) compared to CdS (2.4 eV) should improve the solar cell device efficiency by eliminating absorption loss in the short–wavelength region [7, 43]. Recently thin films solar cell based on chemically bath deposited ZnS(O,OH) buffer layer has been demonstrated to have an 18.5% device efficiency [7].

#### 1.2.4 Deposition methods for ZnS thin films

A variety of methods exist for synthesizing of ZnS thin films. These methods can be divided into physical (sputtering is widely used method), chemical vapor deposition techniques (CVD, ALD) and chemical solution based techniques (CBD, SILAR). Due to ultra high vacuum existing in sputtering systems, high quality, very dense, polycrystalline films (either cubic or hexagonal structures) with  $E_g$  values ranging from 3.59 to 3.72 eV [44-46] could be produced at relatively low temperatures of 200°C [46]. However, chemical methods are more widely used for ZnS thin films deposition. Similar to physical methods, chemical vapor phase techniques can also produce excellent quality, pure, homogeneous, highly transparent and crystalline ZnS films. Well-crystallized hexagonal ( $T_{dep}=400^{\circ}-500^{\circ}$  C) or cubic films ( $T_{dep}=250-350^{\circ}$ C) with high refractive indices of 2.42 (400nm) [47] and  $E_g$  of 3.67 eV [48] were prepared by ALD [47-50]. ZnS thin films having cubic configuration with  $E_g$  of 3.4 and 3.6 eV and refractive indices of 2.19–2.26 were obtained by CVD methods [51-53]. However, vacuum based techniques are slow and rather expensive. Solution based techniques were CBD and SILAR are most commonly used are operated at temperatures of 20–90° C, being as a rule, faster and cheaper. However, ZnS films produced by these methods are usually amorphous or poorly crystalline and non-stoichiometric with some inclusion of oxygen [54-59]. Subsequent annealing procedures are required to improve the crystallinity of the films deposited from solution.

#### 1.2.5 ZnS thin films by CSP

In spite of the number of benefits of CSP method, there were only few papers published on spray-deposited ZnS thin films up to 2003 when we initiated our studies. Chamberlin and Skarman were first who have mentioned already in 1966 the possibility to deposit ZnS thin films by spray pyrolysis [13]. Next work on ZnS thin film deposition was published in 1978 by Ugai et al [9] who had studied sprayed ZnS films deposited from the solution containing zinc acetate or zinc chloride as zinc source and thiocarbamide (tu) as sulfur source at fixed deposition temperature of 450° C. Most of the authors [1, 8, 9, 60] used  $ZnCl_2$  and tu as precursor materials and studied the effect of the deposition temperature on the film structure and optical properties [1, 8, 60]. According to these studies, the films deposited at temperatures below 300 °C were amorphous [1] and those deposited at higher temperatures, up to 550 °C, were polycrystalline with the cubic crystal structure [1, 8, 60]. The films optical transmittance (50–80%) and  $E_g$  (3.3–3.5 eV) values increased with deposition temperature (300–500°C) [1]. As-deposited films were Zn-rich [60] and contain some residues of carbon and chlorine [1]. Post-deposition annealing in air at 500 °C results in formation of ZnO additional phase in the films [1, 8, 60]. The post deposition annealing in  $N_2$  atmosphere at 450 °C [8, 60] or in vacuum at temperatures around 500 °C improves the film crystallinity and promotes the formation of wurtzite structure [1, 60].

According to the above-mentioned studies, deposition of sprayed ZnS films was performed keeping the molar ratio of precursors  $\text{ZnCl}_2$ :tu at 1:1. However, earlier studies on sprayed CdS thin films have demonstrated that CdS formation mechanism involves the formation of the complex between  $\text{CdCl}_2$  and thiocarbamide ( $\text{Cd}(\text{tu})_2\text{Cl}_2$ ) in an aqueous spray solution [15], which decomposes above  $210^\circ\text{C}$  with formation of CdS. In many papers the importance of the precursors molar ratio (Cd/S) in solution and its influence on the films properties have been highlighted [14-17].

Later it was established that  $\text{ZnCl}_2$  and tu form the complex compound dichlorobis(thiourea)zinc with formula  $\text{Zn}(\text{tu})_2\text{Cl}_2$  in an aqueous solution [10- 12, 61, 62]. Detailed studies on structure of  $\text{Zn}(\text{tu})_2\text{Cl}_2$  [63] and its thermal decomposition in different atmospheres are reported [10, 11, 64].

*$\text{Zn}(\text{tu})_2\text{Cl}_2$  as a single source precursor for ZnS films by CSP*

It has been shown that in aqueous solution of  $\text{ZnCl}_2$  and tu form a complex compound, where two thiocarbamide molecules are coordinatively bonded to the zinc ion through the sulfur atom [1]:



Thermal decomposition of  $\text{Zn}(\text{tu})_2\text{Cl}_2$  is an extremely complex process in air and in an inert atmosphere as has been shown by the thermoanalytical studies including evolved gas analysis and characterisation of the solid decomposition products by IR and XRD [10, 11, 64]. In spite of the complexity of the process,  $\text{Zn}(\text{tu})_2\text{Cl}_2$  can be used as a single-source precursor for the deposition of ZnS thin films by CSP. ZnS is formed upon the decomposition of  $\text{Zn}(\text{tu})_2\text{Cl}_2$  already at temperatures slightly above  $200^\circ\text{C}$ . At temperatures higher than  $300^\circ\text{C}$  ZnS crystallises and major part of impurities originated from the ligand expelled at temperatures up to  $400^\circ\text{C}$ . Although the oxidation of ZnS becomes relevant at temperatures higher than  $600^\circ\text{C}$ , ZnO phase, even in low amount, has been detected in the residue of thermal decomposition at temperatures already around  $500^\circ\text{C}$  [10]. It has been shown that ZnO at temperatures around  $500^\circ\text{C}$  originates from  $\text{ZnCl}_2$  [10].

Thus, an extra amount of  $\text{ZnCl}_2$  which remained unbound to the  $\text{Zn}(\text{tu})_2\text{Cl}_2$  complex (the case of 1:1 (Zn:S) spraying solution [1, 8, 60]) may lead to the formation of undesired ZnO phase via the  $\text{ZnCl}_2$  oxidation to oxychloride and its subsequent thermal decomposition.

To summarize, none of the earlier studies has reported the influence of the molar ratio of the precursors on the properties of sprayed ZnS thin films properties. Furthermore, the more extended studies on optical properties including refractive indices studies of sprayed ZnS are missing. The present work constitutes a systematic study on the influence of the precursor molar ratio at different



temperatures on the structural, morphological and optical properties of sprayed ZnS thin films.

### **1.3 ZnO nanostructures**

This chapter begins with a brief introduction to nanostructured materials, their definition and characteristic features. Further, ZnO materials properties, morphology types, possible applications of ZnO nanostructured layers, commonly used preparation techniques and possible growth mechanisms are discussed in more detail.

#### **1.3.1 Introduction to the nanostructures**

Nanostructures could be defined as structures designed on atomic or molecular scale in which at least one dimension is measured in nanometers (1-100 nm) [19]. The interest in these materials has been stimulated by the fact that, owing to the small size of building blocks (particle, grain or layer) and the high surface-to-volume ratio, significant increase in grain boundary area, these materials are expected to demonstrate unique mechanical, optical, electronic, and magnetic properties [18-20]. Due to their superior properties, nanostructured materials find a wide range of applications in novel electronic and optical nanodevices etc. [19, 20]. Controlled and cost-effective fabrication, investigation, and further integration of nanomaterials to nanodevices is a great challenge in nanoscale technology. In particular, ZnO nanostructures have attracted considerable attention over the last years due to their scientific and technological importance. Recently, much effort is being continuously employed in preparation nanostructured ZnO with controlled size and shape [65].

#### **1.3.2 Material properties of ZnO**

Zinc oxide is a wide-bandgap II-VI compound semiconductor. It may have crystal structures of wurtzite, zinc blende or rock salt, which are illustrated in Figure 1.3a, b and c, respectively.

It has been theoretically found that the wurtzite structure is energetically a more favorable structure of ZnO compared to rock salt and zinc blende structures. The zincblende ZnO structure can be stabilized only by the growth on cubic substrates, and the rocksalt (NaCl) structure may be obtained only at relatively high pressures (~10 GPa) [66].

The hexagonal lattice, belonging to the space group  $C6_3mc$ , is characterized by two interconnecting sublattices of  $Zn^{2+}$  and  $O^{2-}$ , in such a way that each  $Zn^{2+}$  ion is surrounded by a tetrahedron of  $O^{2-}$  ions, and vice-versa. The tetrahedral coordination in ZnO results in non-central symmetric structure which subsequently results in strong piezoelectric, pyroelectric effects and spontaneous polarization

and is also a key factor in crystal growth, etching and defect generation [39, 67, 68].

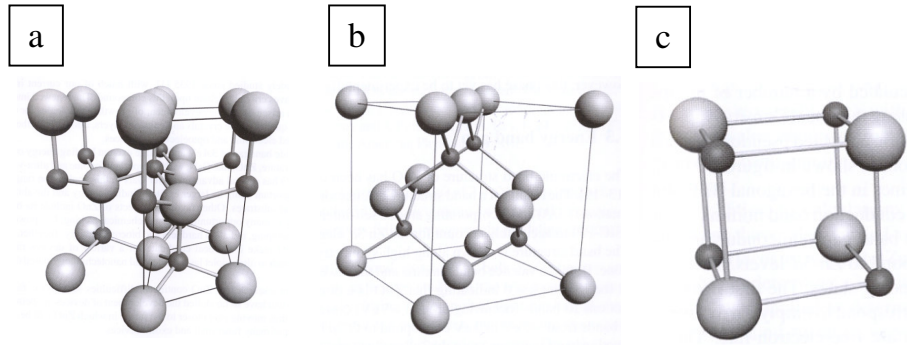


**Figure 1.3** Crystal structures of ZnO a) wurtzite, b) zinc blende and c) rocksalt, O atoms are shown as white large spheres, Zn atoms are small black spheres [39]

Another characteristic feature of wurtzite ZnO is its polar surfaces. The oppositely charged  $O^{2-}$  and  $Zn^{2+}$  ions produce positively charged Zn-[0001] and negatively charged O-[000 $\bar{1}$ ] polar surfaces with maximum surface energy. The surfaces, composed by Zn-O dimers [01 $\bar{1}$ 0], [2 $\bar{1}$  $\bar{1}$ 0] have neutral charge and form non-polar surfaces with energy lower than the [0001] facets. As a result, the growth rate along the [0001] direction is the fastest. Together with the polar surfaces due to atomic terminations, ZnO exhibits a wide range of nanostructures that can be grown by tuning the growth rates along these directions [67].

Figure 1.4 illustrates a few typical growth morphologies of ZnO nanostructures including nanowires, nanorods, nanotubes and nanobelts.

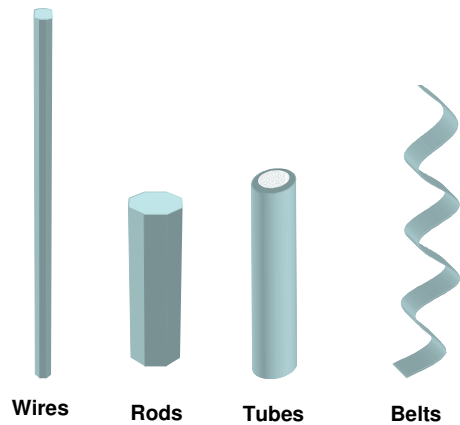


**Figure 1.4** Different morphologies of hexagonal ZnO nanostructures

Table 1.1 summarizes some important physical properties of hexagonal ZnO.

**Table 1.1 Important physical parameters of bulk hexagonal ZnO [28, 69]**

| Properties             | Parameters  |
|------------------------|---|
| Crystal structure      | Wurtzite  |
| Space group            | $P6_3mc$  |
| Lattice constants      | $a=0.324$ nm, $c=0.519$ nm                              |
| Bandgap at 300 K       | 3.37 eV   |
| Refractive index       | $n_o = 1.9985$ , $n_e = 2.0147$ ( $\lambda = 632.8$ nm) |
| Exciton binding energy | 60 meV  |

### 1.3.3 Applications of ZnO nanostructures

The application of nanostructured layers for devices is one of the major focuses of contemporary nanotechnology [22, 23, 67]. Ordered, possessing high surface area ZnO nanostructured layers are expected to enhance the performance of various technologically important devices such as short wavelength lasers, light emitting diodes, Schottky diodes, electroluminescent devices, piezoelectric devices, sensors, and solar cells [21, 22, 70]. There are recently some reports on highly sensitive nanosensors based on ZnO nanorods for detection of hydrogen, ethanol, benzene, and hydrogen sulfide [71-76]. Special interest has arisen to use ZnO nanorods as main component of solar cell devices. Next subchapter describes an idea of using this type of structures in solar cells.

#### *ZnO nanorods for solar cells*

Solar cell is one of the most promising devices in search of sustainable renewable sources of energy. However, current photovoltaic technologies are too expensive to be widely used. Therefore new materials, cost-effective techniques and new approaches are being looked for to significantly improve the cost-performance ratio.

Dye-sensitized solar cell (DSSC), extremely thin absorber (ETA), organic and hybrid organic/inorganic solar cells—are promising devices for inexpensive and large-scale solar energy conversion [21, 77-79].

The schematic illustration of ETA cell is presented in figure 1.5a. Extremely thin absorber solar cell (ETA) and DSSC solar cell are conceptually similar, but instead the extremely thin (<100 nm) layer of inorganic semiconductor used as absorber in ETA cell, dye absorber molecule is used in DSSC. And instead of a void-filling transparent inorganic p-type semiconductor such as CuSCN used in ETA cell, liquid electrolyte solution is utilized in DSSC [80]. One important limiting factor in the nanoparticle-based DSSC and ETA cell performance is electron transport. During its traversal to the photoelectrode, an electron is

estimated to cross  $10^3$  to  $10^6$   $\text{TiO}_2$  nanoparticles, which is crucial for the device performance due to recombination processes. The replacing of the nanoparticle layer by oriented single-crystalline nanorods offers the potential for improved electron transport leading to higher photoefficiencies [77]. Solar cell based on nanorods is illustrated in Figure 1.5b.

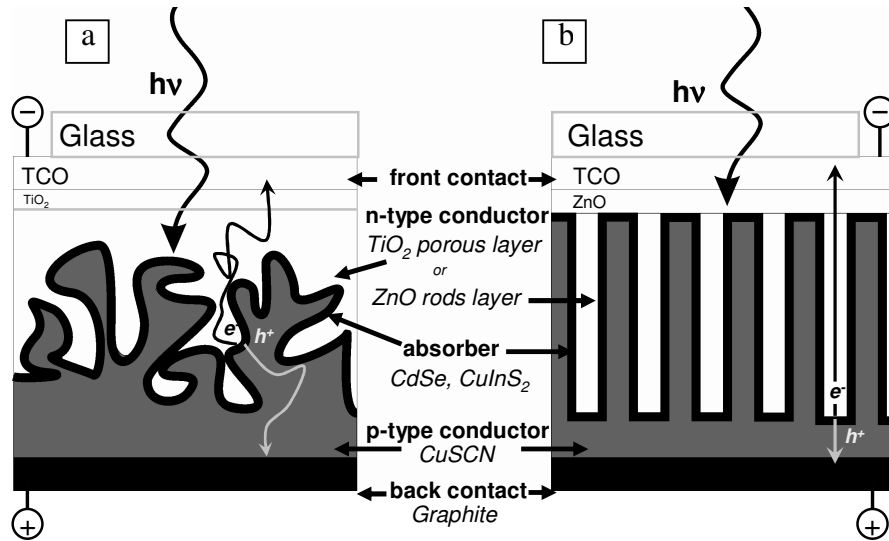


**Figure 1.5** a) Schematic illustration of ETA solar cell based on  $\text{TiO}_2$  layers, b) ETA solar cell based on ZnO nanorods

Very recently promising results with conversion efficiencies of 1.5–2.3% were reported for the  $\text{SnO}_2/\text{ZnO}_{\text{flat}}/\text{ZnO}_{\text{nanorods}}/\text{CdSe}/\text{CuSCN}$  ETA-cells structure by R. Tera-Zaera [81], while an efficiency of 1.69 % with DSSC structure based on ZnO nanorods was achieved by P. Charoensirithavorn and Yoshikawa [79].

### 1.3.4 ZnO films deposition by CSP

ZnO thin films preparation and investigation by spray pyrolysis are the subject of intense research over the years. Enhanced interest in this material has arisen from its possible application as transparent conductive electrode, also in thin film solar cells. There are many published reports on the ZnO thin film deposition by spray pyrolysis [82-87, 88]. Zinc acetate precursor solution and growth temperatures of 300-450° C are typically used to obtain flat films [85-89]. In order to make ZnO films conductive, doping with Al, B, In or Ga is usually applied.

However, there are only a few papers that report the preparation of ZnO films by spraying of  $\text{ZnCl}_2$  solutions [90-92]. The surface of the layers obtained from  $\text{ZnCl}_2$  solution is more textured and rough, films are not conductive and not so transparent compared to those deposited from the acetate precursor. That is why

the  $\text{ZnCl}_2$  precursor for ZnO thin films deposition has not been considered to be of interest. However, one interesting paper on ZnO layers prepared by the CSP technique utilizing  $\text{ZnCl}_2$  solution at  $450^\circ\text{C}$  demonstrated the closed packed crystals with hexagonal facets and pyramidal-like tip ends morphology [91].

To summarize, the studies on ZnO nanorod preparation by CSP appear to be totally missing in the literature.

### 1.3.4 Synthesis methods for ZnO nanostructures

The preparation of ZnO nanorods/nanowires has been demonstrated by various methods. The most common techniques are vapor-liquid-solid (VLS) growth, chemical vapor deposition methods (CVD, MOCVD, PECVD), solution-based techniques (electrodeposition and hydrothermal growth) and template-assisted methods. Short description and comparison of these methods is given below.

#### *Vapor-liquid-solid (VLS) method*

Vapor-liquid-solid growth is the most common method for nanowire and nanorod synthesis. The schematic illustration of VLS growth is presented in Figure 1.6. This method requires a metal catalyst, usually gold (Au) as a seed and besides high deposition temperatures up to  $900\text{--}1100^\circ\text{C}$ . VLS process involves the reduction of ZnO powder by carbon to form zinc and  $\text{CO}/\text{CO}_2$  vapor in the high temperature zone. The zinc vapor is transported into the chamber containing the Au catalysts where it reacts with the Au on silicon substrates, to form liquid alloy droplet. As the droplet become supersaturated, crystalline ZnO nanorods or wires are formed underneath of the droplet [93-96]. The diameter of the nanowire is controlled by the pressure of the vapor [93, 97]. Thus, necessary use of a metal catalyst may contaminate the nanowires and such high processing temperatures are not technologically favorable [98, 99].

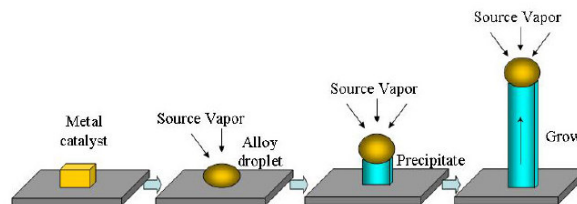


**Figure 1.6 Schematic steps of the growth of a nanowire via VLS process**

#### *Chemical vapour deposition (CVD)*

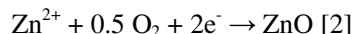
Chemical vapor deposition can be defined as the deposition of a solid layer on a heated surface from a chemical reaction between the precursors in the vapor phase [100].

The precursor compound, most commonly an organic compound which has reasonable vapor pressure is transported by the carrier gas ( $N_2/O_2$ ) into reaction vessel. The reaction proceeds on a substrate surface heated at the growth temperature. The most common CVD techniques used to deposit ZnO nanostructures are thermal CVD, metal-organic CVD (MOCVD) and plasma-enhanced (PECVD) [100]. MOCVD differs from conventional CVD in its choice of metalorganic precursor (for example, diethyl zinc (DEZ)) which have only one dangling bond and can be easily converted to vapors allowing to reduce the growth temperatures [69]. PECVD process utilizes a plasma to enhance chemical reaction rates of the precursors thus reducing the deposition temperatures.

CVD methods can give uniform, conformal and adherent structures, but the disadvantages of these methods are the manipulation of toxic, explosive or corrosive precursors, the use of vacuum and comparatively high temperatures [100].

#### *Electrodeposition (ED)*

Electrodeposition represents a cost-effective and simple solution-based technique. The ZnO deposition occurs on the surface of the working electrode which is immersed into the electrolyte solution (KCl) under applied potential in the course of electrochemical reaction 2 [101-106].



The dissolved molecular oxygen is used as the oxygen precursor. In order to obtain nanostructured ZnO, low concentrations of  $Zn^{2+}$  (5 mmol/l  $ZnCl_2$ ) should be used [102]. The reaction temperatures are in the range of 70-90°C.

Vertically aligned nanowire arrays were synthesised on GaN substrates [102] whereas slightly tilted but elongated rods were grown on  $SnO_2$  and ZnO seeded ITO substrates [102, 106]. The main parameters that control the growth are precursor concentration, applied potential, substrate type, deposition time and current.

#### *Hydrothermal method*

The hydrothermal growth is another low temperature ( $T_d=90-180^\circ C$ ) inexpensive solution-based technique. The hydrothermal growth is performed in a autoclave where the zinc precursor, solvent and substrate (not always) are placed. The reaction occurs under pressure and temperatures above the critical point of the solvent thereby increasing the solubility of a solid and thus speeding up the reaction. This method requires surfactant molecules which regulate the crystal

growth and act as an agglomeration inhibitor. The ZnO seeded substrates are typically used in hydrothermal synthesis. Here, temperature, pressure, deposition time and solution species constitute mainly control the ZnO nanorods synthesis [107- 111].

#### *Template-assisted growth*

In template-assisted method, a highly ordered ZnO nanowire array is formed in a pores of nanoporous template. Alumina membrane (AOO) template is the most commonly used template. Chemical (sol-gel), electrochemical methods and ALD are used to fullfill the pores. After deposition procedure the membrane is dissolved by NaOH. A major limitation of the template-aided synthesis is that the nanowires tend to be polycrystalline due to the heterogeneous nucleation on the pore walls. Removal of the template may cause damage to the nanowires and also introduce impurities such as sodium ions from NaOH into the system. However, it is also difficult to achieve pore diameters of less than 10nm and a pore density exceeding  $10^{16}$  pores/m<sup>2</sup> by this template [112-116].

To summarize, the nanorods can be grown by various methods, vacuum based techniques at high temperatures using CVD or VLS processes or by inexpensive low temperature solution-based techniques such as hydrothermal growth and electrodeposition.

A comparison of deposition methods for ZnO nanorods and nanowires, including their advantages and disadvantages are summarized in Table 1.2.

**Table 1.2 Comparison of preparative methods for ZnO nanorods and nanowires**

| Methods             | T <sub>dep.</sub> °C | ZnO dimensions |       |        | Deposition methods  |  | References     |
|---------------------|----------------------|----------------|-------|--------|---|--|----------------|
|                     |                      | D, nm          | L, μm | L/d    | Advantages  | Disadvantages  |                |
| <b>VLS</b>          | 800-1125             | 30-100         | 1-20  | ...300 | Well-controlled<br>High aspect ratio<br>High c-axis orientation | High growth temperature<br>Contamination by catalyst<br>Nonstoichiometry<br>SA emission in PL spectrum | [93-99]        |
| <b>CVD</b>          | 500-900              | 20-250         | 15    | ...100 | High aspect ratio<br>High c-axis orientation                    | High growth temperature<br>Vacuum, plasma are widely used<br>Volatile and hazardous precursors         | [69, 100, 117] |
| <b>Hydrothermal</b> | 40-110               | 60-200         | ...3  | ...50  | Low temperature<br>Low cost                                     | Long dep.time<br>Random orientation<br>Poor control of parametres<br>SA in PL spectrum                 | [107-111]      |
| <b>ED</b>           | 70-85                | 70-300         | 1.6   | ...23  | Low temperature<br>Low cost<br>Large area                       | SA in PL spectrum<br>Substrate limitation<br>Crystals are not well-faceted                             | [101-106]      |



### 1.3.5 Growth mechanisms of ZnO nanorods and nanowires

The growth mechanism of ZnO nanorods is quite poorly understood and reflected in the literature. The main mechanisms used to explain the formation of ZnO wires (nanorods) are vapor-liquid-solid (VLS), screw dislocations growth, catalyst-free self-nucleation growth and vapor solid (VS) mechanisms, the latter mechanism being mainly applied for nanobelts and thus will not be discussed here [69].

#### *Vapor- liquid -solid (VLS) mechanism*

As it has already been briefly reported above, upon supersaturation of liquid alloy in the VLS method, a nucleation center forms, and serves as a preferred site for the axial growth of a nanowires. The adsorbed gas reactants are then diffused through the liquid phase to the solid/liquid interface, and the growth of the solid phase proceeds. As the liquid surface adsorbs the reactant gaseous species much more efficiently than does the solid phase, the growth is much faster at the solid/liquid interface compared to the solid/vapor interface. The main characteristic of VLS growth is the existence of metallic nanoparticles on top of the nanowires [69].

#### *Screw dislocation mechanism*

In screw dislocation mechanism, structural defects are involved in the process of nanowires (nanorods) formation. When line of a screw dislocation is parallel to the growth axis of the nanowires, the spiral plane perpendicular to the screw dislocation line possesses a low-energy step, which acts as a site sequential growth. Thus, the growth rate along the dislocation line is much faster compared to that in the radial direction. A characteristic of screw dislocation growth is the presence of axial screw dislocations and conically shaped end tips of the nanowires which are evident from high resolution SEM or TEM images [69, 118].

#### *Catalyst-free self-nucleation mechanism*

Another possible mechanism to explain the growth of nanowires (nanorods) with sharp prismatic tips is catalyst-free, self-nucleation growth near equilibrium. When ZnO nuclei have been formed on the surface and have been reached the critical size they begin to grow in all directions. The growth rate relationship for different ZnO crystal faces is  $R_{001} > R_{101} > R_{100}$ . Thus, the growth along the [0001] direction is the fastest. However nanowires (nanorods) attributed to this growth mechanism not only grow in height but also increase in width resulting in sharp prismatic end tips [69].

#### 1.4 Summary of the literature review and aim of the study

The studies reported in the literature on chemical spray pyrolysis deposition of ZnS thin films and ZnO layers can be summarized as follows:

1. Chemical spray pyrolysis deposition is a simple and easily scalable method to prepare large area thin films at low cost. The method is very suitable to prepare high quality zinc oxide thin films. In the case of metal sulfide films a compromise should be made between the content of residues issued from the precursors and oxidation products, which are both controlled by the deposition temperature when proceeds the deposition in air.
2. ZnS thin films by chemical spray method were mainly obtained by deposition of aqueous solutions containing zinc chloride and thiocarbamide as the zinc and sulfur sources, respectively, onto the preheated substrates in the temperature interval of 300-550 °C in air. It has been shown that in an aqueous solution ZnCl<sub>2</sub> and thiocarbamide form the complex compound, dichlorobis(thiourea)zinc. According to the thermoanalytical study, the thermal decomposition of the complex is a multistep process where zinc sulfide is formed in the first decomposition steps at temperatures below 300 °C and, when treated in air, a major part of impurities originated from the precursors are expelled at temperatures around 400 °C. In spite of the fact that the formation of ZnS in CSP process proceeds through the intermediate compound with stoichiometry of ZnCl<sub>2</sub>:tu=1:2, the thin films were mainly deposited using the solution with the precursor molar ratio of 1:1. The studies on the influence of the precursors molar ratio within the different deposition temperatures on the structural, optical and morphological properties of ZnS thin films prepared by CSP are missing in the literature.
3. ZnO nanostructures such as nanorod and nanowire arrays have a wide range of potential applications as solar cells, light emitting diodes, piezoelectric devices, chemical and biological sensors. ZnO layers comprising nanorods are grown by various methods such as vapour-liquid-solid growth, different modifications of chemical vapour deposition, and solution based methods of electrodeposition and hydrothermal growth. ZnO nanorods growth is mainly due to the unique feature of ZnO-wurtzite polar surfaces which ones have maximum surface energy resulting in the fastest growth rate along the hexagonal [0001] direction. There were no reports in the literature demonstrating the possibility or impossibility to grow ZnO nanorods by CSP. ZnO nanostructured layers by cost-effective CSP could be attractive for different applications, including, for example, the new generation nanocomposite solar cells.

Based on the conclusions on deposition of ZnS thin films by CSP and ZnO nanostructured layers, the objectives of the present doctoral thesis were:

1. To deposit ZnS thin films by CSP using aqueous solutions containing zinc chloride and thiocarbamide as starting chemicals. To study the effect of the deposition temperature and molar ratio of the precursors in spray solution on the morphology, composition, structural and optical properties (viz. transmittance, band gap, refractive indices) of spray-deposited ZnS films.
2. To demonstrate the possibility to synthesize ZnO nanostructured layers comprising nanorods by the CSP technique. To deposit ZnO nanorod layers using zinc chloride as a precursor material. To study the influence of the growth temperature and the spray solution variables such as the precursor concentration, type of solvent, additive (thiocarbamide) on the development of ZnO nanorod layers on different substrates. To characterize the ZnO layers morphology, size, shape and quality of ZnO crystals.

## 2. EXPERIMENTAL

### 2.1 Spray pyrolysis deposition procedure

In this work a simple pneumatic spray pyrolysis method has been employed which is described in detail in the section 1.1 for the preparation of ZnS thin films and ZnO nanostructures.

#### 2.1.1 Preparation of ZnS thin films

The ZnS films were prepared using aqueous solutions containing zinc chloride ( $\text{ZnCl}_2$ , Aldrich, 98% purity) and thiocarbamide ( $(\text{NH}_2)_2\text{CS}$ , Merck,  $\geq 98\%$  purity). Deionized water was used as a solvent. Molar ratios of the zinc and sulfur sources were chosen as 1:1, 1:2, 2:1 and the concentration of  $\text{ZnCl}_2$  was kept constant at 0.05 mol/l. Commercial glass slides ( $30 \times 30 \times 1 \text{ mm}^3$ ) and *n*-Si(001) wafers were used as substrates. The deposition temperature was varied from 430 to 600 °C using electronic temperature controller and held constant with an accuracy of  $\pm 10$  °C. The compressed air carrier gas had a flow rate of 8 l/min. The solution spray rate was maintained at 2.5 ml/min [I, II].

#### 2.1.2 Preparation of ZnO nanostructured layers

The ZnO nanostructured layers comprising nanorods were prepared using the aqueous solutions of zinc chloride ( $\text{ZnCl}_2$ , Aldrich, 98% purity). The concentration of  $\text{ZnCl}_2$  was varied from 0.02 to 0.2 mol/l. The studied deposition temperatures on the substrate surface were in the region from 400 to 580°C. For all experiments [III-VI] the solution volume was 50 ml and spray rate was maintained at 2.5 ml/min. Plain glass, two types of ITO/glasses ('fine' and 'large' grained),  $\text{SnO}_2$ -covered glass, ZnO flat 'seed'/glass substrates layers prepared by spraying were used to study the growth of ZnO on different substrates.

For the experiments published in paper [V] alcohol (isopropanol and ethanol) were added to the aqueous solution of  $\text{ZnCl}_2$ .

Nanorods presented in paper [VI] were prepared by mixing the aqueous solutions of  $\text{ZnCl}_2$  and thiocarbamide in molar ratios of Zn:S as 1:0, 1:0.05, 1:0.1, 1:0.25 and 0.5. For these experiments, the concentrations of  $\text{ZnCl}_2$  were chosen as 0.05 mol/l and 0.1 mol/l and the temperature was fixed to 520°C.

### 2.2 Characterisation methods for ZnS thin films and ZnO nanostructured layers

Detailed description of the measurements and the instrumentation used in this study can be found in the experimental sections of Ref. I–VI.

A condensed overview of the characterization methods for ZnS thin films and ZnO nanostructured layers are summarized below in the table 2.1.

**Table 2.1 Methods for characterization of ZnS thin films and ZnO nanostructured layers**

| <b>Material</b> | <b>Properties</b>  | <b>Characterization method</b> | <b>Reference</b> |
|-----------------|--|--------------------------------|------------------|
| <b>ZnS</b>      | Morphology   | SEM                            | I, II            |
|                 | Phase composition  | XRD, FTIR                      | I, II            |
|                 | Structure, grain size, crystallinity                                 | XRD, FTIR                      | I, II            |
|                 | Elemental composition  | EDX                            | II               |
|                 | Optical absorption, transmission, band gap                           | UV-VIS spectrophotometer       | I                |
|                 | Reflectance in IR-region, refractive index                           | FTIR, Ellipsometry             | I                |
| <b>ZnO</b>      | Morphology, crystals size, aspect ratio (L/D), orientation, coverage | SEM, cross-sections            | III-VI           |
|                 | Structure, phase composition, crystallinity                          | XRD, ESB, SAED                 | III, IV, VI      |
|                 | Crystals quality, defects, purity                                    | Photoluminescence              | IV, VI           |
|                 | Optical phonons and lattice modes                                    | Raman                          | V                |

### 3. RESULTS AND DISCUSSION

#### 3.1 Deposition of ZnS thin films by CSP

The following section gives an overview on ZnS thin films prepared by spray pyrolysis based on papers I and II. The structural, phase and elemental composition, morphology as well as optical properties are studied with respect to the molar ratio of the precursors in solution ( $\text{ZnCl}_2$ :tu) and deposition temperatures.

##### 3.1.1 Structure, phase and elemental composition of sprayed ZnS thin films

###### *XRD study*

XRD diffraction patterns of ZnS thin films deposited at different temperatures using solutions with molar ratios of precursors Zn:S 1:1 and 1:2 are presented in Figures 3.1a and b, respectively.

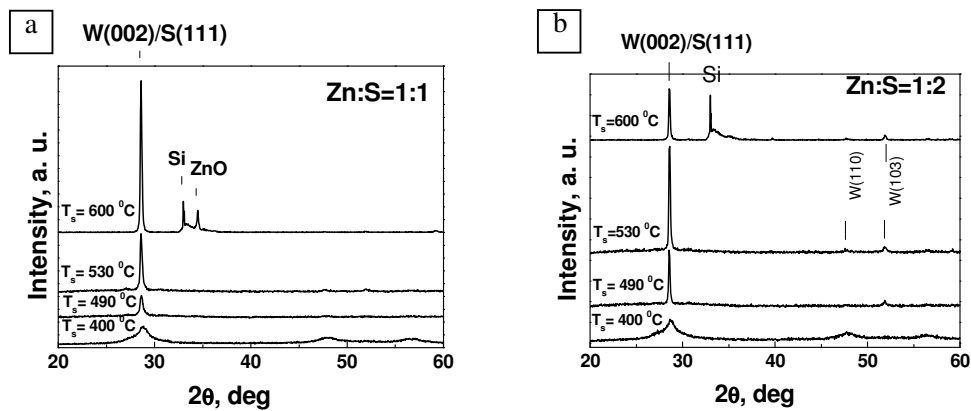


**Figure 3.1** XRD patterns of ZnS films deposited from the solution at different growth temperatures using precursor ratios of Zn:S a) 1:1, b) 1:2

The films grown at  $T_s = 400$ - $530^\circ\text{C}$  were pulverized onto glass substrates, whereas silicon (Si) wafers were used to grow the films at  $600^\circ\text{C}$ . The films deposited at  $400^\circ\text{C}$  and below show poor crystallinity independent of the spray solution composition. Increase in the deposition temperature resulted in sharpening of the main XRD peak at  $2\theta = 28.5^\circ$  indicating improvement of the film crystallinity. XRD patterns of the films deposited from 1:1 and 1:2 solutions are similar up to the deposition temperature of  $530^\circ\text{C}$ . Sharp dominant XRD peak at  $2\theta = 28.5^\circ$  could be assigned to both, the (002) peak of wurtzite (JCPDS 05-0492)

and the (111) peak of sphalerite (JCPDS 05-0566). The films grown at 490 °C have obviously the sphalerite crystal structure as no peaks of wurtzite have been detected. Using the deposition temperature of 530°C, two additional peaks; viz. (002) and (103) of ZnS-wurtzite appear in the X-ray diffractogram of the films obtained from the 1:2 solution, whereas XRD pattern of the 1:1 film remains unchanged. Thus, according to XRD, ZnS-wurtzite films were obtained by spraying 1:2 solutions at growth temperatures above 500 °C, which is significantly lower than 1020 °C reported for sphalerite to wurtzite transition [30, 31]. Moreover, the films from 1:2 solution have better crystallinity as XRD peaks are sharper and more intense compared to those of the films from 1:1 solution. Generally, the increase of the deposition temperature leads to narrower diffraction peaks as seen in the FWHM values, indicating better crystallinity and subsequent increase in the crystallite size. For example, the mean crystallite size in ZnS film from 1:2 solution is 60 nm and 73 nm deposited at 490 °C and 530 °C, respectively, whereas crystallite size of the ZnS obtained from the 1:1 solution at 490 °C is around 30 nm. Consequently, both the growth temperature and molar ratio of precursors have an effect on the crystallite sizes in the sprayed films.

Our results on the formation of ZnS-sphalerite films from the 1:1 solution correspond to the literature data [1, 8, 60]. According to the literature, there were no reports on the formation of ZnS-wurtzite films as we observed using 1:2 spray solution. Even in recently published study, where authors used Zn:S molar ratios from 1:1 to 1:6 in the spray solution, and deposition temperature of 500 °C, the formation of ZnS films with sphalerite structure only has been reported [119]. However there are some reports on formation of ZnS thin films with wurtzite structure at relatively low temperatures compare to the sphalerite-wurtzite transition temperature of 1020 °C [30, 31]. The ZnS films with wurtzite structure were prepared by ALD at 425-500 °C [33, 34] and PVD at 400 °C [35].

Using the deposition temperature of 600° C, the peak of additional ZnO phase appears at  $2\theta=34.82^\circ$  in the XRD pattern of the films prepared from 1:1 solution but was not detected for the films deposited from the 1:2 solution (Figure 3.1 a and b, respectively).

Films deposited utilizing the Zn-rich, 2:1 solutions, showed the replicas of ZnO phase in addition to the main peak of ZnS in a whole deposition temperature interval from 400 to 540° C (Figure 3.2).

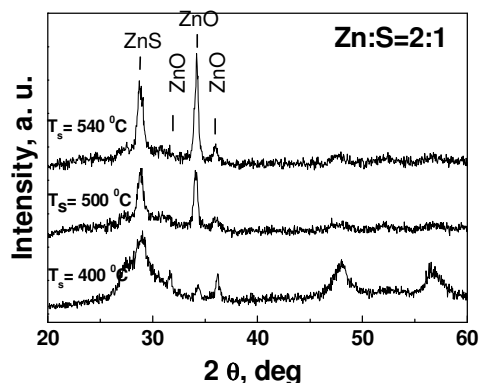


Figure 3.2 XRD patterns of ZnS films deposited from the solution with the precursors ratio of Zn:S=2:1 at different growth temperatures

The 1:1 spraying solution, mainly used to prepare ZnS films by the CSP technique [1, 8, 9] and in particular, 2:1 solution, both contain  $ZnCl_2$  in excess to form the intermediate zinc complex  $Zn(tu)_2Cl_2$  as a precursor for ZnS [10]. Thus,  $ZnCl_2$  originated phases could be present in higher amount and might appear at lower temperatures than in the films produced from 1:2 solutions.

#### FTIR study

According to XRD the films deposited in the temperature interval of 200-380° C were amorphous. These films were characterized by their FTIR spectra recorded in the middle infrared spectral region of 400-4000  $cm^{-1}$ . FTIR spectra of the films deposited from the 1:2 solution at temperatures of 200, 240 and 320° C are presented in Figure 3.3.

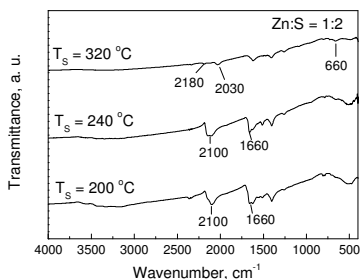


Figure 3.3 FTIR spectra of ZnS films deposited from the solution with the precursors ratio of Zn:S=1:2 at growth temperatures 200°C, 240°C and 320°C

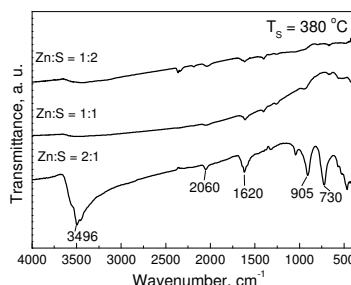


Figure 3.4 FTIR spectra of ZnS films deposited at 380°C using the Zn:S ratio of 1) 1:2, 2) 1:1 and 3) 2:1 in solution



According to FTIR spectra, the films deposited at temperatures 200-320°C contain some residues as thermal decomposition products of the complex compound ( $\text{Zn}(\text{tu})_2\text{Cl}_2$ ). Deposition at 240 °C results in film showing FTIR spectrum similar to that of  $\text{Zn}(\text{tu})_2\text{Cl}_2$  heated up to 230 °C [10]. Strong absorptions close to  $2100\text{ cm}^{-1}$  were observed in the spectra of the films deposited at 200 and 240 °C. These absorptions could be assigned to the thiocyanate ( $\text{SCN}^-$ ) and hydrogen bonded  $\text{RNH}_3^+$  groups, obviously due to the isomerisation of thiocarbamide into ammoniumthiocyanate. FTIR spectrum of the film deposited at 320 °C shows splitting of the double band around  $2100\text{ cm}^{-1}$  into two absorption bands peaked at 2180 and  $2030\text{ cm}^{-1}$ . The absorptions in the region of  $2000\text{-}2200\text{ cm}^{-1}$  and at  $660\text{ cm}^{-1}$  could belong to cyanamide ( $\text{NCN}^{2-}$ ) group; around  $730\text{ cm}^{-1}$  to metal coordinated thiocyanate ion ( $\text{SCN}^-$ ) vibrations, and  $1660\text{ cm}^{-1}$  is characteristic of amide species [120].

FTIR spectra of the 1:1 and 1:2 films deposited at 380°C (Figure 3.4) show only very weak absorptions indicating a significant reduction of organic residues. When the deposition takes place at temperatures higher than 400°C, there are no absorption peaks on the FTIR spectra of the 1:1 and 1:2 films (spectra are not presented).

But FTIR spectrum of the 2:1 film deposited at 380°C differs from those of the 1:1 and 1:2 films (Figure 3.4). Strong absorptions in the regions of  $3200\text{-}3600\text{ cm}^{-1}$  and  $1580\text{-}1690\text{ cm}^{-1}$  appeared in the spectrum, referring to the presence of  $\text{OH}^-$  species and strong contamination of the film by precursor residues.

#### *Elemental analysis*

According to EDX analysis, the Zn/S atomic ratios are 1.01 and 1.11 for the films obtained at 530°C from 1:2 and 1:1 solution, respectively. Thus, slightly Zn-rich films were obtained by spraying of the 1:1 solution being in agreement with the published results [1, 60, 121]. Consequently, another zinc containing phase is present in these films in addition to ZnS. This secondary phase can be zinc oxide, as there is no chlorine or any other contaminants according to EDX which is consistent with FTIR analysis.

Findings, such as that deposition at temperatures close to 500 °C results in Zn-rich films, and the films deposited at 600 °C (Figure 3.1a) or annealed at 450-500 °C in air [1, 8, 60] contain crystalline phase of ZnO, indicate that it is extremely difficult to obtain single-phase ZnS film keeping the  $\text{ZnCl}_2$ :tu molar ratio of 1:1 in spray solution.

The films deposited from 2:1 solution have two areas with different composition as discussed in following section 3.1.2.

### 3.1.2 Morphology of sprayed ZnS thin films

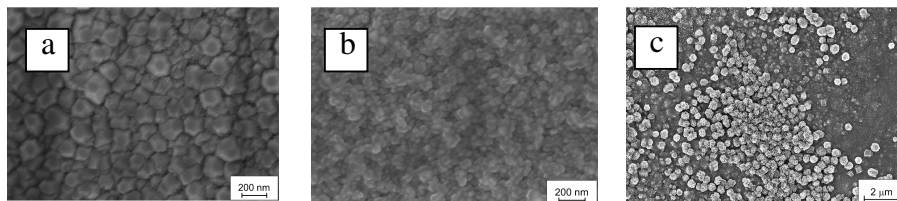


**Figure 3.5** SEM micrographs of ZnS films deposited at  $T_s=500^\circ\text{C}$  using Zn:S ratio of a) 1:2, b) 1:1 and c) 2:1 in the initial solution

SEM micrographs of ZnS films deposited at  $T_s = 500^\circ\text{C}$  using spraying solutions with Zn:S molar ratios of 1:2, 1:1, 2:1 are shown in Figure 3.5 (a-c). The films deposited from 1:1 and 1:2 solutions exhibit uniform surface and dense structure compared to the film obtained from 2:1 solution. ZnS film from the 1:2 solution comprises well-shaped hexagonal prisms with size in the range of 100-180 nm. ZnS film from the 1:1 solution consists of smaller grains with size of about 30 nm. In contrast to these films, the samples from the 2:1 solution possess nonuniform surface with two distinct areas, viz. coalescence of separated crystals and continuous film underneath. According to EDX results, the ratio of Zn/S in these crystals is  $\text{Zn/S} > 10$ , whereas Zn/S ratio in flat area is 1.17. Taking into account EDX and XRD measurements these crystals most probably are composed of the ZnO phase. The flat area is mainly composed of ZnS with some incorporation of ZnO. Most obviously, ZnO phase incorporated into the film was simultaneously formed with ZnS formation from the  $\text{ZnCl}_2$  surplus, and thus is not a product of ZnS oxidation.

### 3.1.3 Optical properties of sprayed ZnS films

#### *Optical transmittance and band gap*

Optical transmittance spectra of ZnS films grown at different temperatures are presented in Figure 3.6.

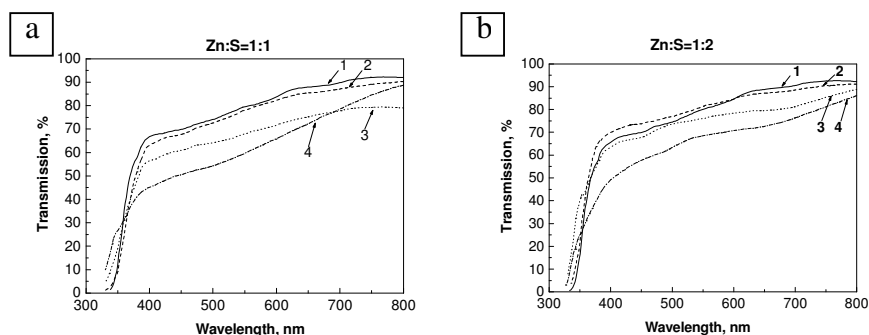


**Figure 3.6** Transmittance spectra of ZnS films deposited at 1) 430, 2) 470, 3) 500, and 4) 530 °C with Zn:S molar ratio in the initial solution a) 1:1 and b) 1:2

The transmittance of the films does not depend much from the molar ration of the precursors in the solution (1:1 or 1:2), but rather decreases with increasing temperature. Such behavior could be explained by increased roughness and light scattering at higher deposition temperatures. Changes in the film morphology and increase of the surface roughness by increasing the deposition temperature is confirmed by SEM study (Figure 3.7).

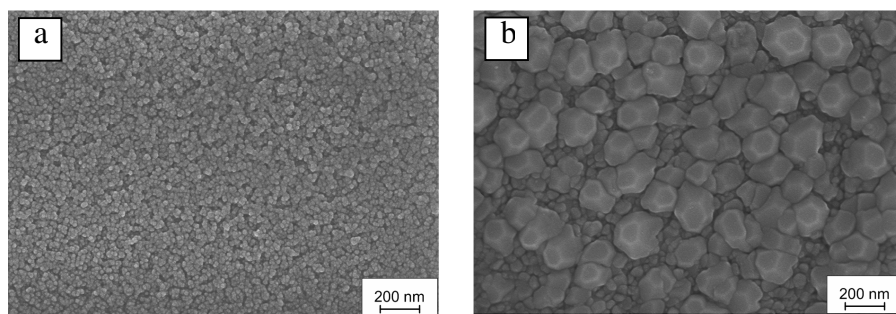


**Figure 3.7** SEM micrographs of the films deposited from 1:2 solution at a) 470 and b) 530 °C

Generally, the ZnS films deposited at 440–500 °C exhibit the transparency higher than 70% in the visible spectral region and 75–90% in the NIR region of 1–2.5  $\mu\text{m}$  (the spectra are not presented). The optical band gap energies ( $E_g$ ) for all the samples were determined from the absorbance spectra (calculation details are given in paper II) and summarized in Table 3.1.

**Table 3.1 Band gap values for the spray-deposited ZnS films**

| $T_s$ (°C) | $E_g$ (eV) |          |
|------------|------------|----------|
|            | Zn:S=1:1   | Zn:S=1:2 |
| 430        | 3.56       | 3.60     |
| 470        | 3.54       | 3.60     |
| 500        | 3.59       | 3.65     |
| 530        | 3.59       | 3.67     |

The band gap values of ZnS films deposited from the 1:1 solution are in the range of 3.54-3.59 eV, being in a good agreement with those reported for the sphalerite ZnS films from 1:1 solution [1, 9]. The band gap energies of ZnS films deposited from the 1:2 solution have larger values, 3.60–3.67 eV. These values correspond to the ZnS bulk with the wurtzite structure [36-38] and are the highest ever reported for sprayed ZnS. The results of a recently published study [119], presenting the  $E_g$  of 3.4-3.6 eV and 3.2 eV for sprayed ZnS films from S-rich and 1:1 solution, respectively, are in agreement with our results.

*Optical reflectance and refractive index*

The reflectance spectra of a bare Si wafer and those of ZnS films deposited on Si, as measured in the NIR region of the spectrum, are shown in Figure 3.8. Reflectivity of silicon wafers ( $R=36\%$ ) was significantly reduced upon the ZnS thin film deposition on it ( $R=10\%$ ). This makes sprayed ZnS applicable as antireflection coatings and components of solar cell.

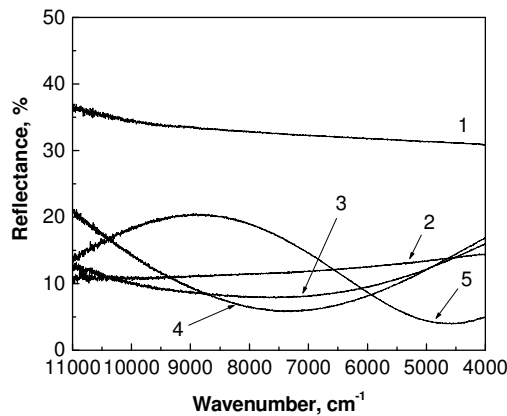


**Figure 3.8 Reflectance spectra of 1) a bare Si substrate and ZnS films on Si, deposited at 2) 460, 3) 500, 4) 540, and 5) 600 °C**

The refractive indices were calculated by two different methods - interference fringe method and ellipsometry. The detailed description of the calculation by fringe method is given in article II.

The values of the refractive indices are summarized in Table 3.2.

**Table 3.2 Refractive indices of sprayed ZnS film**

| Zn:S in solution    | $T_s$ (°C) | Refractive index           |                         |
|---------------------|------------|----------------------------|-------------------------|
|                     |            | Fringe method (NIR region) | Ellipsometry (632.8 nm) |
| 1:1                 | 540        | 1.48                       | NA                      |
|                     | 570        | 1.49                       | NA                      |
| 1:2                 | 540        | 1.82                       | 1.93                    |
|                     | 570        | 1.73                       | 1.77                    |
| * NA – not analyzed |            |                            |                         |

The refractive indices depend on the molar ratio of the precursors. The films prepared from 1:1 solution at temperatures 540–570 °C had refractive indices close to 1.5, whereas the use of the 1:2 spray solution results in the films with higher refractive index typical values being 1.7-1.9 (Table 3.2). A higher refractive index means higher density of the material, indicating better compactness of the 1:2 films. The refractive indices obtained from ellipsometric data, have good correlation with those calculated by the fringe method.

To our knowledge, there are no literature data available on the refractive indices of the ZnS thin films prepared by CSP. Refractive indices of sprayed ZnS films obtained from the 1:2 solution are close to those reported for the ZnS films fabricated by SILAR technique (1.95) [59], being, however, lower than those reported for the ZnS films prepared by ALD (2.46- 2.48) [34] and CVD (2.19-2.26) [52].

### 3.1.4 Conclusions on ZnS thin films

Molar ratio of the precursors in the solution along with the deposition temperature has a significant influence on morphology, structure, composition and optical properties of the ZnS films. ZnS films have hexagonal structure and nearly stoichiometric composition, band gap of 3.67 eV and refractive index up to 1.9 if deposited by CSP using the Zn:S precursors molar ratio of 1:2 in solution and at  $T_s$  close to 530° C.

## 3.2 Deposition of ZnO nanostructured layers by CSP

This section is devoted to a pioneering study on the CSP deposition of ZnO nanostructured layers comprising free-standing ZnO rods. The influence of

deposition parameters such as growth temperature, solution concentration, substrate type, usage of organic solvent or thiocarbamide additive on formation and development of ZnO nanostructured layers has been mainly followed by SEM. Crystal quality of sprayed ZnO nanostructures has been controlled by PL and Raman spectroscopies, as well as SAED.

### 3.2.1 Effect of the deposition temperature

The influence of the substrate temperature on the ZnO layers morphology has been investigated in papers [III] and [IV]. Samples discussed in paper III were deposited using glass substrates and ZnCl<sub>2</sub> concentration of 0.1 mol/l, whereas more diluted solutions with concentration of 0.05 mol/l were used to grow ZnO nanorods on ITO covered glass substrates [IV].

Development of ZnO films surface morphology as a function of the deposition temperature is illustrated in Figure 3.9 (a-d).

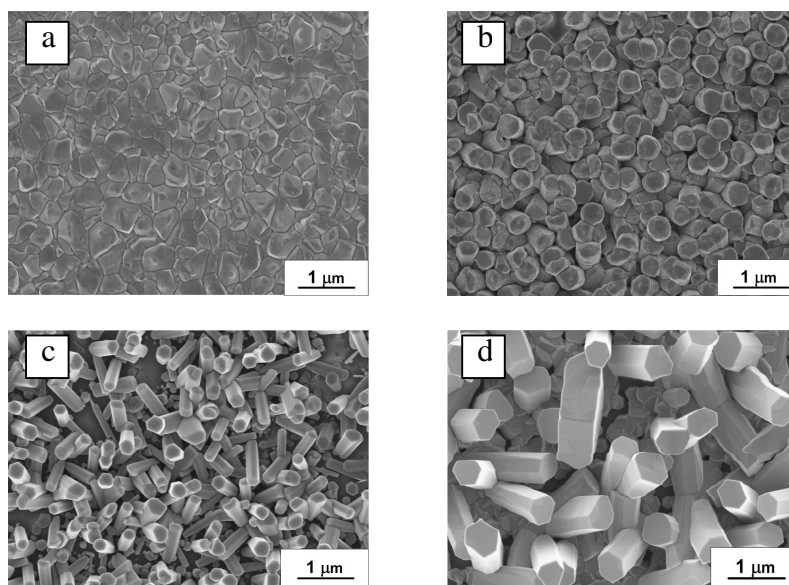


**Figure 3.9 SEM surface views of ZnO layers deposited from zinc chloride aqueous solutions with concentration of 0.1 mol/l onto glass substrates at temperatures ( $T_s$ ) of a) 400 °C, b) 450 °C, c) 490 °C and d) 540 °C**

With an increase of the deposition temperature flat and dense films develop into structured layers. At deposition temperature of 400° C (Figure 3.9a) the film consisting of densely packed grains with a size from 50 up to 500 nm has been formed. The film deposited at 450 °C is no longer compact consists of cylindrical crystals with a diameter of 300 nm (Figure 3.9b). Higher deposition temperature of 490 °C results in formation of separate well-shaped and elongated hexagonal ZnO

crystals with diameter in the range of 200-300 nm and length of 700-800 nm (Figure 3.9c). And, finally, at 540 °C the rods with diameter of 400-600 nm (Figure 3.9d) and length of up to 2.0 μm have been grown. Thus, as expected, the dimensions of the rods have been increased with increasing the growth temperature. The results of the SEM study are summarised in Table 3.3.

**Table 3.3** The ratio of intensities of the (002) and (101) reflections ( $I_{002}/I_{101}$ ) in the XRD pattern and the diameter (d), length (L), aspect ratio (L/d) of ZnO nanorods on glass substrates as a function of the deposition temperature ( $T_s$ ). Concentration of  $ZnCl_2$  in spray solution was 0.1 mol/l

| $T_s$ , °C | $I_{002}/I_{101}$ | d, nm   | L, nm     | L/d   |
|------------|-------------------|---------|-----------|-------|
| 450        | 7.7               | 500     | ~1000     | 2     |
| 490        | 8.6               | 200-300 | 700-800   | 2.5-4 |
| 540        | 6.0               | 400-600 | 1500-2000 | 2-4   |

The XRD patterns of all above mentioned samples – the flat films and structured layers – were similar. Figure 3.10 represents the XRD pattern of ZnO structured layer deposited at 490°C. Strong and narrow, intense XRD peak at  $2\theta = 34.82^\circ$  corresponds to the (002) plane of wurtzite (JCPDS 36-1451), weak reflections of the (101) and (102) planes of the wurtzite can be seen as well. The ratio of the intensities of (002) and (101) reflections ( $I_{002}/I_{101}$ ) of this sample is 8.6. For comparison, the  $I_{002}/I_{101}$  ratio of a powder sample is only 0.4 [JCPDS 36-1451]. The  $I_{002}/I_{101}$  of the structured samples prepared at different temperatures is presented in Table 3.3. According to XRD, the ZnO nanorod layers are highly crystalline, and the crystals are strongly oriented along the c-axis, perpendicular to the substrate.

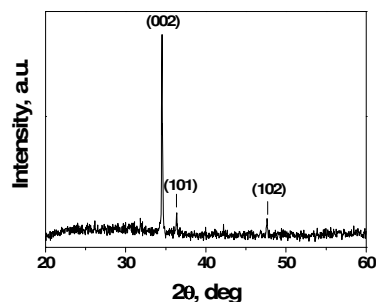


**Figure 3.10** XRD spectrum of the ZnO layer deposited at 490 °C onto a glass substrate using  $ZnCl_2$  with concentration of 0.1 mol/l

The development of ZnO nanostructures comprising nanorods on ITO substrates is similar to that observed on the glass substrates. Compact film develops into a porous layer at temperatures 450 °C and elongated well-shaped hexagonal prisms with diameter in the range of 100-200 nm and length of 800-900 nm (aspect ratio 4-9) are formed at 580 °C (Figure 1 in IV). The XRD pattern of the ZnO nanorod layers on ITO substrate is similar to the XRD pattern of samples deposited on glass indicating high crystallinity and strong c-axis orientation ( $I_{002}/I_{101} \sim 10$ ). The mechanism how the highly c-axis orientated ZnO flat films develop into mainly c-axis orientated ZnO nanocolumns by increasing the growth temperature is not yet clear. To some extent, it can be compared to nanorods growth in the MOCVD process [122]. Both technologies are characterised by the c-axis anisotropic growth of ZnO at higher temperatures. In the MOCVD process, ZnO gradually evolves from flat to pillar and finally to needle-shape crystals by changing the growth temperature in the range of 300-600 °C [122]. In the spray process, a flat film evolves also into nanocolumns but both, rod diameter and length on glass substrates increase with the increasing temperature.

ZnO layers deposited at temperatures above 450 °C are hazy and show considerably lower perpendicular optical transmittance than the compact films (Figure 1 in Ref. III). This behaviour could be explained by the light scattering from the rough surface.

Thus, temperature has a strong influence on the ZnO layer morphology. The well-shaped elongated ZnO nanorods can be prepared by spray of zinc chloride solutions at temperatures ~ 490 °C and higher, whereas at lower temperatures ZnO compact layers are formed.

### **3.2.2 Effect of the precursor concentration**

The effect of precursor concentration on ZnO layer morphology, structure and orientation was studied in papers III and V.

To study the effect of solution concentration on the ZnO formation, the growth temperature was fixed at 560 °C. Concentration of  $ZnCl_2$  has a significant influence on the size, shape and orientation of the ZnO nanorods. Figure 3.11 shows the SEM images of the samples fabricated on glass substrates using different precursor concentrations from 0.02 to 0.2 mol/l.



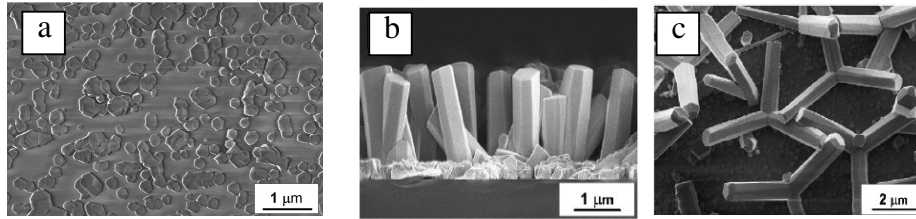


**Figure 3.11 SEM micrographs of the ZnO layers deposited at substrate temperature of 560 °C onto glass substrates using zinc chloride solutions with concentrations of a) 0.02 mol/l, b) 0.1 mol/l and c) 0.2 mol/l**

The dimensions, aspect ratio and ratio of intensities of the XRD (002) to (101) reflections of ZnO nanorods depending on the precursor concentration in solution are summarized in Table 3.4.

**Table 3.4 The ratio of intensities of the XRD (002) and (101) reflections ( $I_{(002)}/I_{(101)}$ ), the diameter (d), length (L), aspect ratio (L/d) of ZnO nanorods deposited at 560 °C on glass substrates using different zinc chloride concentrations in solution (C)**

| C, mol/l | $I_{(002)}/I_{(101)}$ | d, nm   | L, nm     | L/d   |
|----------|-----------------------|---------|-----------|-------|
| 0.02     | N/A                   | 200-400 | 200       | 1-0.5 |
| 0.05     | 9.0                   | 100-300 | ~1500     | 5-15  |
| 0.10     | 5.5                   | 400-600 | 2000-2500 | 3-6   |
| 0.20     | 1.3                   | 600-700 | ~3000     | 4-5   |

Low concentration of  $ZnCl_2$  (0.02 mol/l) in spray solution leads to the formation of flat and thin, platelets-like separate crystals on a glass substrate (Figure 3.11a). The use of more concentrated solutions of 0.05 or 0.1 mol/l results in elongated, almost vertically standing crystals. The dimensions of the rods deposited from 0.1 mol/l solutions are nearly two times larger than those grown from  $ZnCl_2$  concentration of 0.05 mol/l. For instance, diameter of ZnO rods obtained from 0.05 mol/l solution is in the range of 100-300 nm and length up to 1.5  $\mu m$ , whereas diameter of the crystals deposited from 0.1 mol/l is 400-600 and length of 2-2.5  $\mu m$  (Table 3.4). Further increase of the solution concentration from 0.1 to 0.2 mol/l results not only in a larger crystal dimensions (see Figures 3.11b and 3.11c, respectively, and Table 3.4), but also in the change of crystals orientation. Sets of branched, tripod-shaped crystals are formed by spraying of 0.2 mol/l solution (Figure 3.11c). Each crystal in the bundle has uniform size and exhibits well-shaped planes of the hexagonal structure. The crystals are oriented in different directions having nearly equal angle ( $\sim 120^\circ$ ) between of each other and are slightly tilted from the substrate surface. According to XRD studies, (Table 3.4, Figure 3.3 in III) the  $I_{002}/I_{101}$  of these samples has decreased to 1.3 indicating a change in crystal orientation. Thus, SEM and XRD both demonstrate a decreased c-axis orientation of the columns on glass substrates when more concentrated solutions

are sprayed. Similar tripod-like structures with poor substrate coverage, as presented in Fig 3.11c, have been prepared by hydrothermal and plasma-enhanced CVD techniques onto bare Si wafers [123, 124]. The formation of ZnO nanotetrapods, having four crystals in a bundle, is reported by VLS process [125].

To summarize, the concentration of precursor solution has a profound influence on the crystal dimensions, shape, coverage and orientation. Highly c-axis oriented ZnO nanorods could be obtained by spraying ZnCl<sub>2</sub> solutions with concentrations of 0.05 – 0.1 mol/l. Branched tripod-like crystals are formed using the concentration of 0.2 mol/l on glass substrate.

### 3.2.3 Effect of the substrates

The influence of different substrate types and their morphology on ZnO nanorods growth is investigated in papers III, IV and V. It is well-known that the substrate surface morphology is highly important for the nucleation and subsequent growth of the crystals. It has been reported that highly c-axis orientated and uniform in size rods can be produced on substrates with a high density of nuclei by hydrothermal growth [126 - 128], and most frequently conductive substrates (ITO, SnO<sub>2</sub>/covered glasses) should be used for application purposes. The SEM cross-sectional image of spray deposited ZnO rods on the ITO covered glass substrates is presented in Figure 3.12.

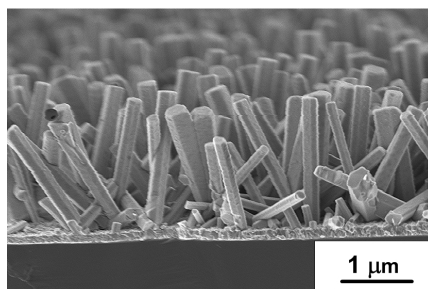


**Figure 3.12 SEM micrograph of ZnO layers deposited onto ITO substrate at 560 °C from zinc chloride solutions with concentration of 0.1 mol/l**

It can be seen that rods with diameter between 70-200 nm and length of ~ 2 μm, resulting in the aspect ratio of 10-30 have been formed on ITO substrate using ZnCl<sub>2</sub> concentration of 0.1 mol/l. Particularity of the nanorods deposited on ITO compared to those grown on bare glass substrates (Figure 3.9 and 3.11) are more regular and uniform size and have smaller diameters, better orientation, and higher substrate coverage. This could be explained by the absence of nucleation sites on bare glass concerned to the high number of nuclei on crystalline ITO or SnO<sub>2</sub> substrate.

However, the ITO layer may have different morphology. In our study, presented in paper IV, we have tested ITO –covered glasses with two different types of

morphology. ITO, named type A, presented in Figure 3.13a, has a rough surface with pyramid-like grains, whereas ITO, so-called, type 'B' has fine-grained microstructure as illustrated in Figure 3.13b.

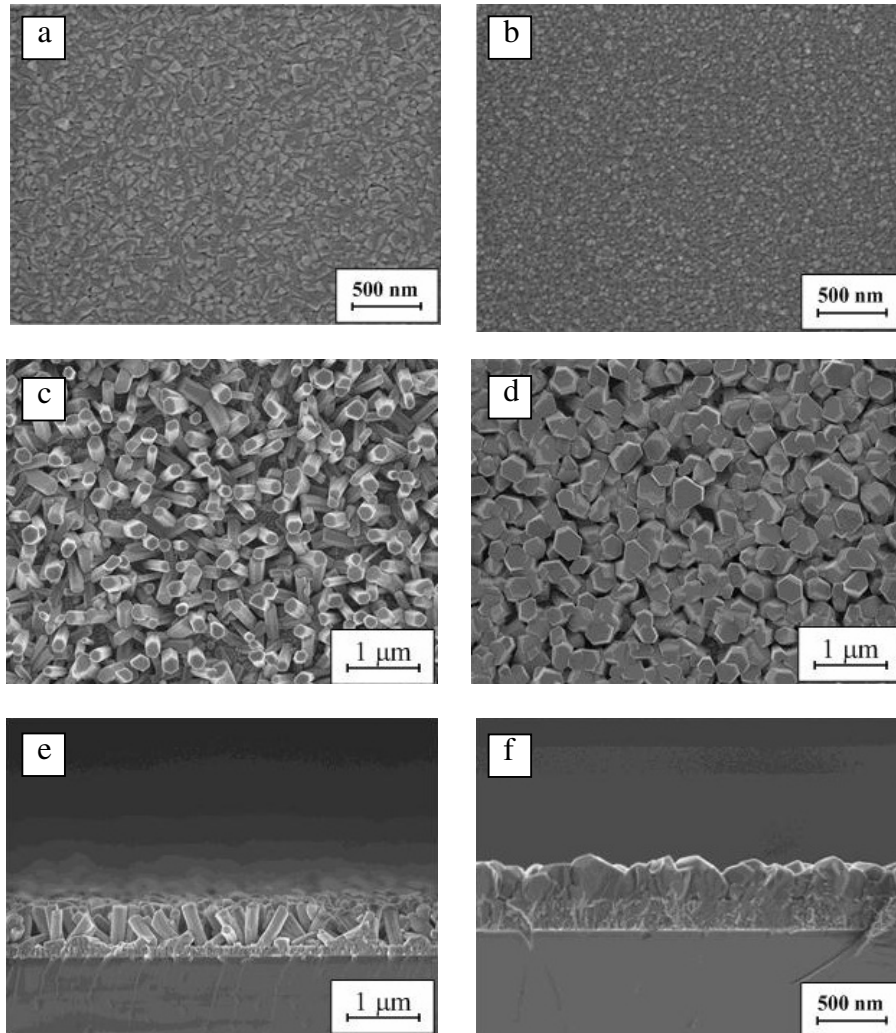


**Figure 3.13 SEM micrographs: a) surface view of ITO- type A (,large grain'); b) plane view of ITO- type B (,small grain'); c) a surface view and e) a cross-sectional view of ZnO layers deposited onto the ITO-type A; d) a surface view and f) a cross-sectional view of the layers deposited onto the ITO –type B. ZnO layers (c, d, e, f) were deposited at  $T_s=560\text{ }^\circ\text{C}$  using zinc chloride aqueous solution with concentration of 0.05 mol/l**

The ZnO rods formation was observed only on ITO with larger grains and rough surface (type A, Figure 3.13c). Using fine-grained ITO (type B), the layer of densely packed fat ZnO crystals (Figure 3.13f) has been formed. Similar results were shown for RF sputtered ZnO on a copper seed layer covered glass substrates [129]. ZnO nanorod growth was observed on granular copper, whereas ZnO film was obtained on smooth seed layer.

The density of nuclei in B-type ITO is definitely much higher compared to large-grained ITO and thus, the number of crystals formed in an early stage of the growth can also be high. Obviously, the coalescence of next to each other crystals occurs during the growth resulting in the compact ZnO layer as shown in Figures 3.13d and 3.13f.

The SnO<sub>2</sub> is an important TCO material and is widely used as solar cells electrode. In this work we have found that the ZnO nanorods growth onto SnO<sub>2</sub> covered glass substrates is similar to that observed on ITO-covered substrates. The nanorods are well-aligned perpendicular to the substrate and substrate coverage is high. But due to higher number of nuclei on ITO or SnO<sub>2</sub> substrates than on glass, the precursor solution shouldn't be concentrated. For instance spray of ZnCl<sub>2</sub> with 0.2 mol/l lead to the formation of compact layer (Figure 4b in V). In order to obtain nanorods on conductive substrates the concentrations of the precursors should be 0.05-0.1 mol/l in case of ITO and below 0.1 mol/l in case of SnO<sub>2</sub>.

In order to initiate the nucleation and growth of well-aligned ZnO nanorods in some studies so called thin 'seed' layer, typically ZnO, is deposited on a substrate first [106, 130, 131,]. In our study published in paper V ZnO layers with rough surface (similar to ITO large grained surface) and ZnO smooth films have been sprayed onto glass substrates prior the ZnO nanorods deposition. The ZnO structured layer comprising rods was formed on a 'rough' spray-deposited ZnO layer only [V, Figure 2b]. In the case of ZnO film with smooth surface, hexagonal crystals with diameter of 400 nm and low aspect ratio (less than 1) were formed [V, Figure 2c].

To conclude, the ZnO nanorods could be grown on different types of substrates, such as glass, ITO, SnO<sub>2</sub> and sprayed ZnO film on glass. More uniform, highly c-axis oriented elongated ZnO nanorods grow preferably on conductive electrode substrates (ITO, SnO<sub>2</sub>). Due to the high number of nucleation sites on ITO and SnO<sub>2</sub> substrates, in order to avoid coalescence of the crystals, the concentration of precursor solution (ZnCl<sub>2</sub>) should not exceed 0.1 mol/l [V].

### 3.2.4 Effect of solvent and additive

#### *Effect of solvents*

It is well-known that alcoholic solvents are the most preferred in spray deposition process because they facilitate the formation of smaller droplets due to low surface tension and viscosity [2]. Most of the sprayed ZnO thin films have been deposited with an addition of alcohol to precursor solution [88]. In the present study, which is

published in paper V, we used solvents containing isopropyl alcohol and ethanol. SEM microphotos of ZnO layers on glass substrates obtained from alcoholic and aqueous solutions with ZnCl<sub>2</sub> concentration of 0.1mol/l are presented in Figures 3.14a and 3.14b, respectively.

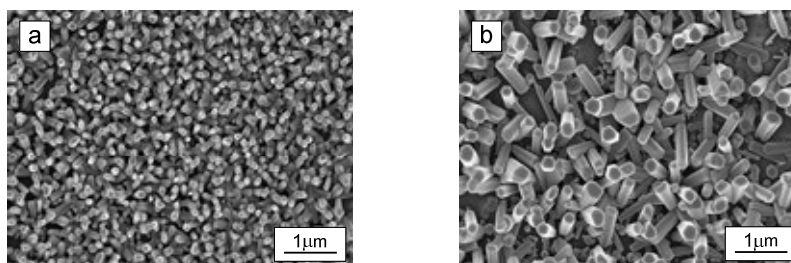


**Figure 3.14 SEM photos of ZnO nanorods on glass substrates obtained from a) alcoholic and b) aqueous solutions, ZnCl<sub>2</sub> concentration 0.1 mol/l, Ts=510 °C**

A comparison of diameters, lengths, aspect ratios and density of the rods grown at Ts=510 and 550 °C using only water and water with addition of alcohol is summarized in Table 3.5.

**Table 3.5 Diameters (d), lengths (L), aspect ratios (L/D) and density of ZnO rods deposited from aqueous and alcoholic solutions with the precursor concentration of 0.1 mol/l at Ts=510 °C and 550 °C**

|                                       | Ts=510° C |               | Ts=550° C |               |
|---------------------------------------|-----------|---------------|-----------|---------------|
|                                       | Water     | Water+alcohol | Water     | Water+alcohol |
| d, nm                                 | 200-300   | 70-80         | 300-400   | ~150-200      |
| L, nm                                 | 900       | 600           | 2000      | 1000          |
| L/D                                   | 3-4.5     | 7-8           | 5-7       | 5-7           |
| Density of rods, rods/μm <sup>2</sup> | ~10       | ~40           | ~2        | ~11           |

The ZnO nanorods prepared from alcoholic solution are noticeably thinner, showing higher aspect ratios and better substrate coverages compared to those deposited from aqueous solutions.

#### *Effect of the thiocarbamide in the spray solution on ZnO nanorod morphology and crystal properties*

In this section we present the results on the formation of ZnO nanorods prepared by spraying aqueous solutions containing ZnCl<sub>2</sub> and thiocarbamide (tu) at different molar ratios. It has been observed that addition of thiocarbamide into the spray

solution has great impact on the size, shape and phase composition of the ZnO crystals. This study is published in paper VI.

### *Morphology*

SEM images of ZnO nanorods deposited onto SnO<sub>2</sub> substrates from two types of solutions: (1) zinc chloride and (2) zinc chloride mixed with thiocarbamide (Zn:tu =1:0.25) are presented in Figure 3.15a and 3.15b, respectively.

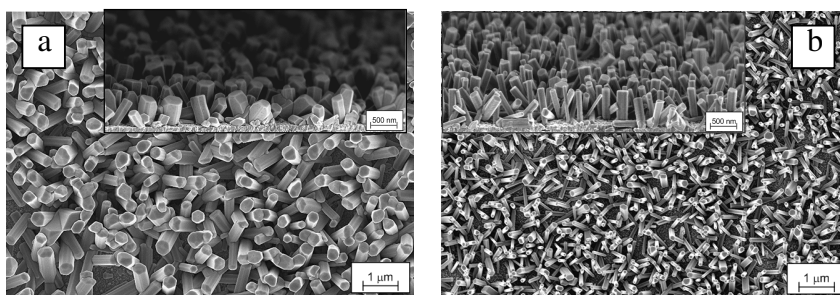


**Figure 3.15 SEM micrographs showing the surface and cross-sectional views (inset) of ZnO samples deposited onto SnO<sub>2</sub> substrate at Ts=520°C using ZnCl<sub>2</sub> aqueous solutions: a) without and b) containing thiourea at Zn:tu molar ratio of 1:0.25; [Zn<sup>2+</sup>]=0.05 mol/l**

The diameters of rods decreased from 300 to 120 nm, and length increased from 500 to 700 nm, resulting in more than three-fold increase of the aspect ratio for the samples deposited from thiourea-containing solution. Even at higher concentration of ZnCl<sub>2</sub> solution (0.1 mol/l) with small addition of tu (Zn:tu=1:0.25) elongated highly orientated ZnO nanorods are formed with high aspect ratio (~12) (Figure 1 in VI).

### *Phase composition*

According to XRD analysis, the ZnO nanorods obtained by spraying the solution containing zinc chloride and thiocarbamide at Ts=520°C are highly crystalline without any impurity phases (Figure 3 in VI), similarly to the nanorods deposited from ZnCl<sub>2</sub> solution.

However, some “spots” like contaminations on the side facets of well formed hexagonal crystals were observed in high magnification SEM image (Figure 3.17b).

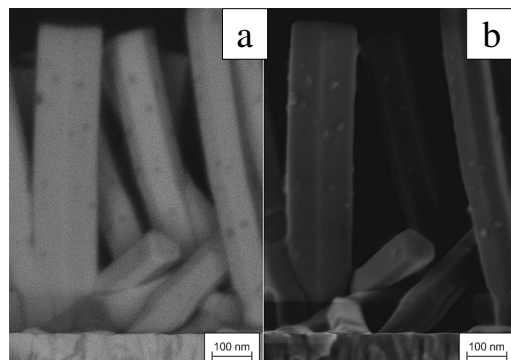


**Figure 3.16** a) ESB and b) high magnification SEM cross-sectional micrographs of the sample deposited by spraying the solution containing  $\text{ZnCl}_2$  and thiocarbamide ( $\text{Zn:tu}=1:0.25$ ),  $[\text{Zn}^{2+}]=0.1\text{mol/l}$ ,  $T_s= 520^\circ\text{C}$

The colour contrast difference on ESB analysis (Figure 3.17a) clearly indicates that the elemental composition of ‘spots’ differ from that of the ZnO rods. As it has been shown in part 3.1 of the thesis, chemical spray deposition of  $\text{ZnCl}_2$  and thiourea solution at around  $500^\circ\text{C}$  results in ZnS thin films. To control whether the “spots” belong to ZnS phase, the ZnO sample with higher content of tu in solution was prepared (molar ratio of  $\text{Zn:tu}= 1:0.5$ ). XRD pattern of this sample, recorded at parallel beams (Figure 3.17) indicated weak reflection at  $2\theta$  of  $28.5^\circ$ , which could be attributed to the (111) reflection of ZnS sphalerite phase (JCPDS 05-0566)

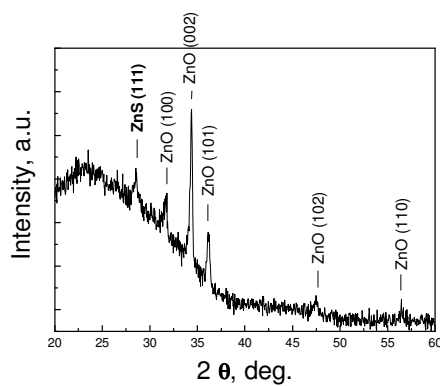


**Figure 3.17** XRD pattern of the sample obtained from solution containing  $\text{ZnCl}_2$  and thiocarbamide ( $\text{Zn:tu}=1:0.5$ ),  $[\text{Zn}^{2+}]=0.1\text{ mol/l}$ . Diffractogram was recorded using X-ray parallel beam

### Growth mechanism

To understand the growth mechanism of ZnO nanorods obtained by spraying ZnCl<sub>2</sub> solutions with and without thiocarbamide addition their morphologies in the different growth stages were examined by SEM (Figure 6a-f in VI).

Already after one minute deposition time, elongated small crystals appeared on the substrate from thiourea containing solutions (Figure 6b, VI), while hardly any crystals were seen on a substrate from ZnCl<sub>2</sub> solution (Figure 6a, VI). After 5 and 15 minutes deposition time spraying of ZnCl<sub>2</sub> solution resulted in a thicker rods whereas giant crystals have been formed using thiourea containing solution (Figure 6c-d, VI). On the basis of the SEM, ESB and XRD results we propose the model of possible mechanism for of the ZnO nanorod formation of without and in the presence of thiourea as illustrated in Figure 3.18.

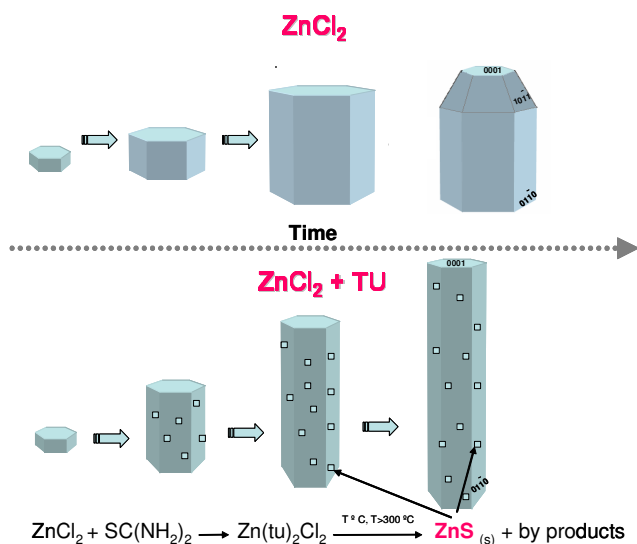


**Figure 3.18 Schematic illustration of the possible growth mechanism for the formation of ZnO nanorods by spraying ZnCl<sub>2</sub> solutions without and with thiourea**

It is known that in some crystallization processes the growth rate of a crystal facet can be inhibited by the addition of an impurity strongly adsorbing onto the growth front [132]. Here we propose that the ZnS particles, originated from the zinc-thiocarbamide complex decomposition are adsorbed onto the freshly formed ZnO side facets retarding the lateral growth and promoting this way the longitudinal growth (Figure 3.18). As a result thinner high aspect ratio rods are formed. Similar growth mechanism preventing the “width” growth and facilitating



the c-axis growth has been observed for ZnO nanorod formation in chemical bath deposition process using hexamine and oleic acid additives [133, 134].

Thus, the dimensions of the ZnO rods by CSP could be easily controlled by presence of solvents or some additives in the precursor solutions. It was found that thiocarbamide additive promotes the longitudinal growth resulting in thinner high aspect ratio ZnO rods. Presence of organic solvents in the solution leads to the formation of noticeably smaller rods and higher coverage of the substrates.

### 3.2.5 Properties of spray-deposited ZnO nanorods

The crystalline quality of sprayed ZnO nanorods was tested by SAED, PL and Raman spectroscopy measurements. The results on these measurements are summarized in this section and have been published in papers I-VI of the thesis.

#### *SAED*

According to SAED pattern (Figure 3.21), each individual nanorod is a single crystal, independent of the growth temperature and solution concentration.

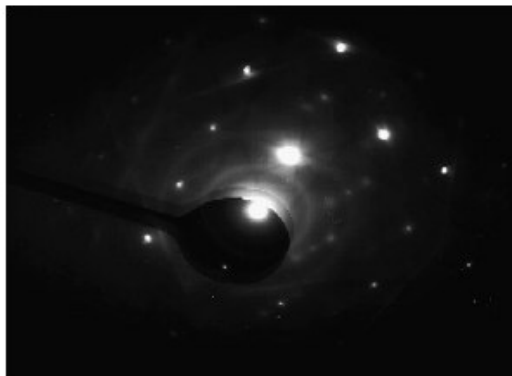


**Figure 3.21** Selected area electron diffraction (SAED) pattern of a single ZnO nanorod grown from ZnCl<sub>2</sub> solution at Ts=490°C

#### *PL properties of ZnO nanorod layers*

Room-temperature PL spectra of the samples deposited from the ZnCl<sub>2</sub> solutions and ZnCl<sub>2</sub> mixed with thiourea (Zn:tu =1:0.25) at Ts =520°C are presented in Figure 3.22.

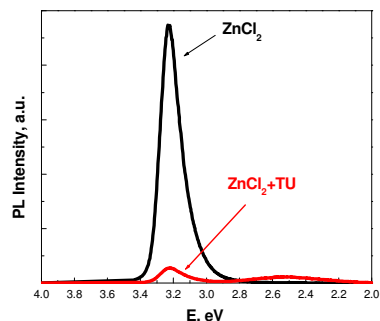


**Figure 3.22** Room-temperature PL spectra of the ZnO nanorods prepared from solutions of  $\text{ZnCl}_2$  and  $\text{ZnCl}_2$  containing thiocarbamide at molar ratio of  $\text{Zn:tu}=1:0.25$ ,  $[\text{Zn}^{2+}]=0.05$  mol/l  $T_s=520$  °C

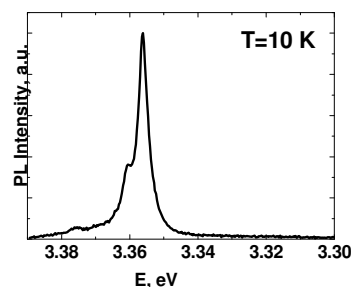


**Figure 3.23** High-resolution PL spectra of ZnO nanorod layers deposited at  $T_s=560$  °C

PL spectra of ZnO nanorod samples measured at room temperature and at 10 K are presented in Figures 3.22 and 3.23, respectively. For ZnO nanorod layers obtained by spraying the  $\text{ZnCl}_2$  solution, strong near band edge (NBE) emission, characteristic of pure material, is the dominant band in PL spectra. In the room-temperature PL spectrum, the NBE band is wide and centered close to 3.2 eV. High-resolution PL measurements at 10 K reveal the dominant NBE emission peaks at 3.360 eV and 3.356 eV with the FWHM of 4-5 meV, and a weak emission at 3.375 eV. The dominant emissions could be assigned to the exciton transition bound to neutral donors (DoX) [135] and the peak at 3.375 eV to the free-exciton emission. Deep level emission peaked at 2.4 eV, generally attributed to the presence of oxygen vacancies and associated with the structural defects, was not detected in the PL spectra of sprayed ZnO nanorod layers obtained from  $\text{ZnCl}_2$  solution. Thus, compared to low temperature wet chemical methods used for the growth of ZnO nanorods [128-136], the sprayed ZnO nanorods possess higher optical and crystalline quality.

The ZnO nanorods prepared from solution containing thiocarbamide resulted in lowered NBE emission peak with appearance of weak broad SA band at 2.4 eV (Figure 3.22) indicating lower crystalline quality compared to the samples prepared from  $\text{ZnCl}_2$  solution.

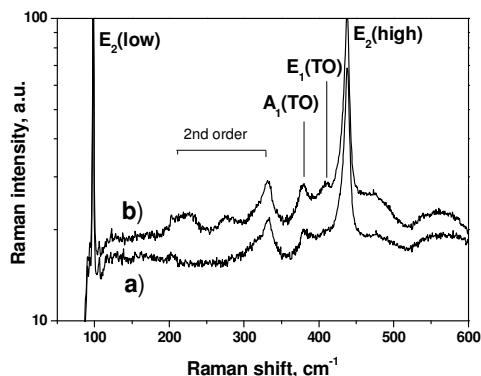


**Figure 3.24** Sprayed ZnO nanorod layers Raman spectra from samples composed of a) nearly vertically standing ZnO rods (SEM micrographs are presented in Figures 3.12b); b) tripods (SEM micrograph is presented in Figure 3.12c)

Figure 3.24 shows the Raman spectra of ZnO layers composed of well c-axis orientated ZnO rods (curve a) and of tripods (curve b). Strong Raman bands at 99 and 438  $\text{cm}^{-1}$  were observed for both samples. These bands correspond to ZnO nonpolar optical phonon  $E_2$  (low) and  $E_2$  (high) modes of hexagonal wurtzite phase respectively and are characteristic of high crystal quality wurtzite [137, 138]. The FWHM of the  $E_2$  (high) mode at 438  $\text{cm}^{-1}$  of sprayed ZnO nanorods is around 6  $\text{cm}^{-1}$  and comparable to 8  $\text{cm}^{-1}$  of ZnO nanowires [139]. The small difference in the spectra is the presence of vanishingly weak peak of  $E_1(\text{TO})$  band at 410  $\text{cm}^{-1}$  for the tripod-like ZnO layers (Figure 3.24b). The  $E_1(\text{TO})$  mode is sensitive to the orientation of nanostructure. This mode is detected from the tilted nanowires and randomly oriented nanobelts and cannot be usually observed from the vertically aligned nanowires [138, 140].

In summary, according to PL and Raman measurements, the ZnO nanorods prepared from  $\text{ZnCl}_2$  solution by spray pyrolysis possess excellent optical quality and high purity. The SAED studies demonstrated that individual nanorod is single-crystalline. The sample prepared from solution with addition of thiocarbamide is not so pure but probably contaminated by impurities originated from thiourea.

## CONCLUSIONS

### *ZnS thin films*

The phase composition, crystallinity, morphology and optical properties of ZnS thin films prepared by chemical spray pyrolysis technique using aqueous solutions of zinc chloride and thiocarbamide are controlled by both growth temperature and the precursor molar ratio in spraying solution.

1. The films deposited at temperatures of 240-380 °C are amorphous and contain high amount of residues originated from the precursors. Using growth temperatures above 400 °C, major part of impurities are expelled and the films become crystalline.
2. Highly (002) oriented ZnS films with the wurtzite structure and closely stoichiometric composition could be grown at 500-600 °C in air using the 1:2 molar ratio of precursors ( $\text{ZnCl}_2$  and  $\text{SC}(\text{NH}_2)_2$ ) in the spraying solution. ZnS films from the 1:1 solution have dominantly sphalerite structure, Zn-rich composition and contain ZnO as secondary phase at growth temperatures close to 600 °C. Films obtained from Zn-rich solution (Zn:S=2:1) have nonuniform surface and composition consisting of mixture of ZnS and ZnO phases.
3. The band gap and refractive indices of the ZnS films prepared by spray of 1:2 solution are higher (Eg of 3.67 eV and  $n=1.82$  (at 632.8 nm)) compared to those obtained from the 1:1 solution (Eg of 3.59 eV and  $n=1.48$  (at 632.8 nm)). Sprayed ZnS films exhibit optical transparency in the order of 70-80 % in the visible spectrum region and demonstrate antireflective coating properties reducing the reflectivity of Si wafers from 36% to 10%.

### *ZnO nanostructured layers*

1. ZnO nanostructured layers comprising nanorods can be grown by a simple and cost-effective chemical spray pyrolysis technique using zinc chloride as precursor. The morphology of ZnO layers, dimensions and orientation of nanorods, substrate coverage and quality of the crystals are controlled by growth temperature, precursor concentration, substrate type and additives in the solution.
2. Compact ZnO films develops to the structured layers when the growth temperatures of 450°C and higher are used. Well-shaped highly crystalline hexagonal ZnO rods with preferred c-axis orientation on a substrate could be grown at temperatures around 550 °C using  $\text{ZnCl}_2$  concentrations of

0.05-0.1 mol/l in the spray solution. Higher concentrations of  $\text{ZnCl}_2$  ( $c=0.2$  mol/l) lead to the compact layer formation in the case of deposition on TCO substrates and ZnO tripods-like crystals development on glass substrates. The diameter of the rods could be decreased and aspect ratio increased using alcohol-based solvents or small addition of thiourea into the  $\text{ZnCl}_2$  solution ( $\text{Zn:S} = 1:0.25$ ).

3. ZnO nanorods prepared by chemical spray of zinc chloride solutions are of high optical and crystalline quality single crystals as confirmed by Raman and PL spectroscopic studies and selective area electron diffraction measurements.

## ACKNOWLEDGEMENTS

This thesis is based on the experimental work carried out during 2003-2007 in the Laboratory of Semiconductor Materials at the Materials Science Department, Tallinn University of Technology.

Above all, I would like to express my deepest gratitude to my supervisor – Research Professor Malle Krunk for her excellent guidance, support and encouragement during this work.

I would like to express my special thanks to the unique person who unfortunately is not anymore among us – Prof. Peter Enn Kukk for showing me the entrance door to the Laboratory of Semiconductors Materials and the Head of the Department of Materials Science, Professor Enn Mellikov for opening this door and giving me the possibility to carry out the present study.

I owe my gratitude to the co-authors and colleagues at the Department of Materials Science. Special thanks are due to Dr. Arvo Mere for teaching me the optical and electrical measurements, being always ready to help and to answer any questions; Atanas Katerski for keeping the instruments working and always helping should a need arise, Olga Volobujeva and Dr. Valdek Mikli for SEM, EDX and SAED studies, Maarja Grossberg for PL measurements, and others for their friendship and support.

I am also deeply thankful to my former teacher and advisor Dr. Mare Altosaar, who is greatly contributing to my knowledges on semiconductor materials both in theory and in practice.

I am very grateful to the opponents - Prof. Lauri Niinistö and Dr. Thierry Pauporté - for their valuable time and comments.

Most importantly, my heartfelt thanks belong to my family, especially, to my husband Andrei for his invaluable support and encouragement during this work.

And finally, financial support from the Estonian Science Foundation grants No. 5612 and 6954, Estonian Ministry of Education and Science target financing project 0142515s03SF and Estonian Doctoral School of Materials Science and Materials Technology (MMTDK) are gratefully acknowledged. This support enabled attendance in International Scientific Conferences.

Tallinn, December 2007

Tatjana Dedova

## ABSTRACT

### Chemical Spray Pyrolysis Deposition of Zinc Sulfide Thin Films and Zinc Oxide Nanostructured Layers

This thesis is focused on the studies on chemical spray pyrolysis deposition of ZnS thin films and ZnO nanostructured layers consisting of nanorods.

The properties of ZnS thin films were studied, dependent on the molar ratio of precursors ( $\text{ZnCl}_2$  : tu) in solution and growth temperature ( $T_s = 230\text{--}600$  °C) by means of various techniques including XRD, SEM, EDX, FTIR, UV-VIS and ellipsometry. It was found that the phase composition, crystallinity, structure, morphology and optical properties of sprayed films are controlled by both the substrate temperature and molar ratio of precursors in the solution.

The films deposited at temperatures below 400 °C were amorphous and contaminated by the residues originating from the precursors. Films became crystalline if deposited at temperatures around 400 °C or above. Slightly Zn-rich ( $\text{Zn/S}=1.11$ ) films with the sphalerite structure were grown in the temperature interval of 490-530°C using the precursor molar ratio of 1:1, whereas the films from 1:2 solution at  $T_s=530^\circ\text{C}$  were highly oriented wurtzite having nearly stoichiometric composition ( $\text{Zn/S}=1.01$ ). Additional ZnO phase was detected on the diffractogram of 1:1 film deposited at  $T_s=600^\circ\text{C}$  while this phase was not detected in the XRD patterns of the films deposited from the 1:2 solution at this temperature. Films utilizing the 2:1 solution were Zn-rich ( $\text{Zn/S}=\text{up to } 10$ ) with ZnO phase incorporation even at low deposition temperatures ( $T_s=400\text{--}540^\circ\text{C}$ ).

Refractive indices and band gap values were higher for the ZnS films deposited at  $T_s=530^\circ\text{C}$  from the 1:2 solution ( $n=1.8$  at 632.8 nm and  $E_g=3.67$  eV compared to those obtained from the 1:1 solution ( $n=1.5$  at 632.8 nm and  $E_g=3.59$  eV). All films independent of the molar ratio demonstrated high optical transmittance (70-80 %) in the visible and infrared spectral region and reduced the reflectivity of Si wafers from 36% to 10% thus showing their applicability as antireflection coatings in devices.

The second part of the thesis was focused on the deposition of ZnO nanorod layers by chemical spray pyrolysis technique. The ZnO layer formation, composition, structure, morphology, dimensionality and orientation of the ZnO crystals as well as optical properties were investigated with respect to growth temperature, solution concentration, substrate type (glass, ITO,  $\text{SnO}_2$ , ZnO seed layer) and presence of additives (solvents, thiocarbamide) in the spraying solution. SEM, XRD, SAED, PL and Raman spectroscopic measurements were carried out to characterize the ZnO layers.

Dense ZnO thin films formed at temperatures around 400 °C were transformed to highly structured layers at temperatures around 450 °C or above. Well-shaped highly crystalline hexagonal ZnO rods with preferred c-axis orientation on glass or on transparent conductive oxide covered substrates could be grown at temperatures

around 550 °C using ZnCl<sub>2</sub> concentrations of 0.05-0.1 mol/l in the spraying solution. The concentration of 0.2 mol/l results in branched and tilted crystals, mainly tripods on glass substrates while compact ZnO layer formation was observed on conductive electrode substrates. Generally, the nanorods deposited onto TCO substrates had more regular and uniform sizes, smaller diameters, better orientation perpendicular to the substrate and higher substrate coverage compared to those grown on bare glass. The addition of organic solvent (ethanol or isopropanol) into the spraying solution supported the development of significantly smaller rods (d=70-80 nm, L=600 nm) in comparison to the rods obtained from purely aqueous solutions (d=200-300 nm, L=900 nm). Furthermore, in this study it was found that small additions of thiocarbamide into spraying solution of ZnCl<sub>2</sub> (ZnCl<sub>2</sub> :tu =1:0.25) promoted the development of significantly thinner ZnO nanorods with a higher aspect ratio.

According to the PL and Raman studies, ZnO nanorods, deposited from the ZnCl<sub>2</sub> solutions are of high optical and crystalline quality. According to SAED each separate nanorod is a single crystal. The results obtained, together with simplicity and low cost of the spray procedure, make the technology promising for preparation of ZnO nanorods which are applicable in nanodevices.



## KOKKUVÕTE

### Tsinksulfiidi õhukesed kiled ning tsinkoksiidi nanostruktuursed kihid keemilise pihustuspürolüüsi meetodil

Käesolev doktoritöö on pühendatud tsinksulfiidi õhukeste kilede ja tsinkoksiidi nanostruktureeritud, nanovarrastest koosnevate kihtide kasvatamisele keemilise pihustamise meetodil.

Uuriti pihustatud ZnS kilede omadusi sõltuvalt kasvatamise temperatuurist vahemikus 230–600 °C ja lähteainete (ZnCl<sub>2</sub> ja tiokarbamiid) kontsentratsioonide molaarsuhtest lahuses. Kilede uurimiseks kasutati XRD, SEM, EDX, FTIR, UV-VIS ja ellipsomeetria mõõtmismeetodeid. Kasvutemperatuuridel alla 400 °C sadestatud kiled sisaldavad olulisel määral tsinktiokarbamiidkloriidi laguprodukte ja on halva kristallilisusega. Kristallilised kiled saadi kasvatamisel 400 °C juures ja sellest kõrgematel temperatuuridel. Kiled, mis kasvatati temperatuuridel üle 500 °C, ei sisaldanud enam lähteainetest tulenevaid lisandeid. Kasutades ekvimolaarset (1:1) pihustuslahust ja sadestustemperatuure 490–530 °C, saadakse kuubilise struktuuriga Zn-i rikkad kiled (Zn/S=1.11), mis kõrgemal kasvutemperatuuril (600 °C) sisaldavad kristallilist ZnO faasi. Kilede sadestamisel 500–600 °C juures tsinkkloriidi ja tiokarbamiidi molaarsuhtel 1:2 saadi heksagonaalse struktuuriga ligikaudu stöhhiomeetrilise koostisega (Zn/S=1.01) ZnS kiled, mis on c-telje suunas tekstureeritud. Kiled, mis saadi lähtelahuste molaarsuhtel 2:1, on tsingi rikkad ja sisaldavad lisaks ZnS-le ka ZnO faasi.

ZnS kiled, mis sadestati 1:2 lahusest 530 °C juures, omavad suuremat keelutsooni laiust ja murdumisnäitajat kui 1:1 lahusest valmistatud kiled. Näiteks 1:2 ja 1:1 lahustest kasvatatud kilede murdumisnäitajad on vastavalt 1.8 ja 1.5 (632.8 nm juures) ning keelutsooni laiused vastavalt 3.67 ja 3.59 eV. Pihustatud ZnS kiled omavad 70–80 %-list optilist läbilaskvust nähtavas ja infrapunases spektri osas. Leiti, et pihustatud ZnS kiled vähendavad oluliselt valguse peegeldumist räni pinnalt ja seega võivad leida kasutamist ka odavate antireflektoorse katetena.

Teine osa doktoritööst käsitleb ZnO nanovarrastest koosnevate kihtide kasvatamist keemilise pihustamise meetodil. Kirjanduse andmetel ei ole ZnO nanovardaid varem keemilise pihustamise meetodil saadud. Tsinkoksiidi nanostruktureeritud kihtide moodustumist ZnCl<sub>2</sub> lahuste pihustamisel, sealhulgas kihtide faasikoostist, struktuuri, morfoloogiat, kristallide mõõtmeid ning orienteeritust kihis uuriti sõltuvalt kasvatamise temperatuurist, lähtesoola kontsentratsioonist pihustuslahuses, aluse tüübist (klaas; ITO, SnO<sub>2</sub> ja ZnO-ga kaetud klaas) ja lisanditest pihustuslahuses. Kihte uuriti SEM, XRD, SAED, Raman ja PL spektroskoopia meetoditega. Ilmnes, et sadestustemperatuuri tõstmisel üle 450 °C muutub sile, kompaktne ZnO kile struktureeritud kihiks, mis koosneb eraldi seisvatest heksagonaalsetest kristallidest. Hästi väljakujunenud heksagonaalse struktuuriga tsinkoksiidi nanovardad moodustuvad kasvatamisel 550

°C juures kasutades  $\text{ZnCl}_2$  kontentratsioone pihustuslahuses 0.05-0.1 mol/l. Kõrgema kontsentratsiooniga lahuste (0.2 mol/l) pihustamisel moodustuvad klaasalustele tripoodide-kujulised kristallide kogumikud, kusjuures juhtiva oksiidiga kaetud aluste (TCO) puhul kujunes välja kompaktne ZnO kiht. Üldiselt, TCO peale sadestatud nanovardad on ühtlasema mõõduga, väiksema diameetriga, parema c-teljelise orienteeritusega ja annavad aluse parema kattetiheduse kui klaasile kasvatatud nanovardad. Kasutades lahustina alkohole moodustuvad tunduvalt väiksemad ZnO nanovardad ( $d=70-80$  nm,  $L=600$  nm) kui samadel tingimustel vesilahustest pihustatud kristallid ( $d=200-300$  nm,  $L=900$  nm). Väikese koguse tiokarbamiidi lisamine pihustuslahusesse ( $\text{ZnCl}_2$  :tu =1:0.25) viis tunduvalt peenemate ja suurema kuvasuhtega nanovarraste moodustumisele. PL ja Raman spektroskoopia ning SAED analüüsi tulemused näitavad, et keemiliselt pihustatud ZnO nanovardad on puhtad, kõrge kvaliteediga monokristallid. Saadud tulemused koos keemilise pihustuspürolüüsi lihtsuse ja odavusega näitavad, et see tehnoloogia on paljulubav nanoseadiste jaoks vajalike omadustega ZnO nanovarraste valmistamiseks.

## REFERENCES

1. B. Elidrissi, M. Addou, M. Regragui, A. Bougrine, A. Kachouane and J. C. Bernède. Structure, composition and optical properties of ZnS thin films prepared by spray pyrolysis. – *Materials Chemistry and Physics*, 2001, 68, p. 175–179.
2. P.S. Patil. Versatility of chemical spray pyrolysis. – *Materials Chemistry and Physics*, 1999, 59, p. 185–198.
3. C.H. Chen, F.L.Yuan and J. Schoonman. Spray pyrolysis routes to electroceramic powders and thin films. – *European Journal of Solid State Inorganic Chemistry*, 1998, 35, p. 189–196.
4. L. Niinistö, Development and analytical characterization of thin film electroluminescent devices: An integrated approach. – *ANNALI DI CHIMICA*, 1997, 87, p. 221–232.
5. O.L. Arenas, M.T.S. Nair and P.K. Nair. Chemical bath deposition of ZnS thin films and modification by air annealing. – *Semiconductor Science Technology*, 1997, 12, p. 1323–1330.
6. A. Malik, A. Sêco, E. Fortunato and R. Martins. New UV-Enhanced Solar Blind Optical Sensors based on Monocrystalline Zinc Sulphide. – *Sensors and Actuators A*, 1998, 67, p. 68–71.
7. R. N. Bhattacharya and K. Ramanathan. Cu(In,Ga)Se<sub>2</sub> thin film solar cells with buffer layer alternative to CdS. – *Solar Energy*, 2004, 77, p. 679–683.
8. H. H. Afifi, S. A. Mahmoud, and A. Ashour. Structural study of ZnS thin films prepared by spray pyrolysis. – *Thin Solid Films*, 1995, 263, p. 248–251.
9. A. Ugai, V.N. Semenov, E.M. Averbakh. ZnS–CdS thin films deposition by spray pyrolysis. – *Izvestija Akademii Nauk SSSR, Neorganicheskie Materiali (In Russian)*, 1978, 14, p. 1529–1530.
10. M. Krunk, J. Madarász, T.Leskelä, A. Mere, L. Niinistö and G. Pokol. Study of zinc thiocarbamide chloride, a single-source precursor for zinc sulfide thin films by spray pyrolysis. – *Journal of Thermal Analysis and Calorimetry*, 2003, 72, p. 497–506.
11. J. Madaraz, P. Bombiz, M. Okuya and S. Kaneko. Thermal decomposition of thiourea complexes of Cu, Zn, Sn, chlorides as precursors for the spray pyrolysis decomposition of sulphide thin films. – *Solid State Ionics*, 2001, 141–142, p. 439–446.
12. J.M. Alia, H.G.M. Edwards and M. Stoev. A systematic FT-Raman spectroscopic study of twelve bis-thiourea complexes, A(tu)<sub>2</sub>B<sub>2</sub>. – *Spectrochimica Acta A*, 1999, 55, p. 2423–2435.
13. R.R. Chamberlin and J.S. Skarman. Chemical spray deposition process for inorganic films. – *J. Electrochem. Soc.* 1966, 113, p. 86–89.
14. J. B. Mooney and S. B. Redding. Spray pyrolysis processing. – *Annual Review Materials Science*, 1982, 12, p. 81–101.

15. M. Krunk, J. Madaraz, L. Hiltunen, R. Mannonen, E. Mellikov and L. Niinistö. Structure and thermal behaviour of Dichloro-Bis(Thiourea)Cadmium(II), a single-source precursor for CdS thin films. – *Acta Chemica Scandinavica*, 1997, 51, p. 294–301.
16. M. Krunk, E. Mellikov and E. Sork. Formation of CdS films by spray pyrolysis. – *Thin Solid Films*, 1986, 145, p. 105–109.
17. M. Krunk, E. Mellikov and E. Sork. CdS formation under thermal decomposition of interaction products of thiourea with CdCl<sub>2</sub>. – *Zurnal Neorganicheskoi Khimii* (in Russian), 1985, 30, p. 1373–1376.
18. H. S. Nalwa. Nanostructured materials and nanotechnology. San Diego (Calif.): Academic Press, 2002. 834 p.
19. P. Yang. The chemistry of nanostructured materials. New York: World Scientific, 2003. 386 p.
20. M.C. Roco, R.S. Williams and P. Alivisatos. Nanoparticles and nanotechnology research. – *Journal of Nanoparticle Research*, 1999, 1, p. 1–6.
21. A. M. Peiro, P. Ravirajan, K. Govender, D. S. Boyle, P. O'Brien, D. D. C. Bradley, J. Nelson and J. R. Durrant. The effect of zinc oxide nanostructure on the performance of hybrid polymer/zinc oxide solar cells. – *Journal of Materials Chemistry*, 2006, 16, p. 2088–2096.
22. Y. Xia, P. Yang, Y. Sun, Y. Wu, B. Mayers, B. Gates, Y. Yin, F. Kim and H. Yan. One-dimensional nanostructures: synthesis, characterization and applications. – *Advanced Materials*, 2003, 15, p. 353–389.
23. Y. Wang, W. Chen, Q. Luo, S. Xie and C.H. Chen. Columnar-grown porous films of lithium manganese oxide spinel prepared by ultrasonic spray deposition. – *Applied Surface Science*, 2006, 252, p. 8096–8101.
24. M. S. Tomar and F. J. Garcia. Spray pyrolysis in solar cells and gas sensors. – *Crystal Growth Characterization*, 1981, 4, p. 221–248.
25. G. Cao. Nanostructures and nanomaterials: synthesis, properties and applications. London: Imperial College Press, 2004. 451 p.
26. H.L. Tuller. Oxygen ion and mixed conductors and their technological applications. Boston: Kluwer Academic Publishers, 2000. 473 p.
27. N. Golego. Thin film polycrystalline TiO<sub>2</sub> by spray pyrolysis. – Ph.D. Thesis, 1998, University of Guelph, Canada.
28. W. Kiyotaka, K. Makoto and A. Hideaki. Thin film materials technology – Sputtering of Compound Materials. New York: William Andrew Publishing, 2004. 531 p.
29. H. M. Pathan and C. D. Lokhande. Deposition of metal chalcogenide thin films by successive ionic layer. – *Bulletin of Materials Science*, 2004, 27, p. 85–111.
30. S. D. Scott and H. L. Barnes. Sphalerite-wurtzite equilibria and stoichiometry. – *Geochimica et Cosmochimica Acta*, 1972, 36, p. 1275–1295.

31. B. Gilbert, B.H. Frazer, H. Zhang, F. Huang, J.F. Banfield, D. Haskel, J.C. Lang, G. Srajer and G. De Stasio. X-ray absorption spectroscopy of the cubic and hexagonal polytypes of zinc sulfide. – *Physical Review B*, 2002, 66, p. 2452051–2452056.
32. R. D. Pike, H. Cui, R. Kershaw, K. Dwight, A. Wold, T. N. Blanton, A. A. Wernberg and H. J. Gysling. Low temperature preparation of zinc sulfide thin films by ultrasonic spray pyrolysis from Bis(diethylthiocarbamate)Zinc(II). – *Thin Solid Films*, 1993, 224, p. 221–226.
33. J. A. Lahtinen, A. Lu, T. Tuomi and M. Tammenmaa. Effect of growth temperature on the electronic energy band and crystal structure of ZnS thin films grown using atomic layer epitaxy. – *Journal of Applied Physics*, 1985, 58, p. 1851–1853.
34. M. Oikkonen. Comparison of ZnS thin films grown by ALE zinc acetate and zinc chloride an x-ray diffraction and spectroscopic ellipsometric study. – *Materials Research Bulletin*, 1988, 23, p. 133–142.
35. Z.-J. Xin, R. J. Peaty, H. N. Rutt and R. W. Eason. Epitaxial growth of high-quality ZnS films on sapphire and silicon by PLD. – *Semiconductors Science Technology*, 1999, 14, p. 695–698.
36. M.Y. Nadeem, W. Ahmed and M.F. Wasiq. ZnS thin films – an overview. – *Journal of Research (Science)*, 2005, 16, p. 105–112.
37. V.I. Gavrilenko, A.M. Grehov, D.V. Korbutjak and V.G. Litovchenko. *Optical Properties of Semiconductors Handbook*. Kiev: Naukova Dumka, 1987. 392 p.
38. <http://en.wikipedia.org/wiki/ZnS>. Date 10.09.2007.
39. C. Jagadish and S. J. Pearton. *Zinc oxide bulk, thin films and nanostructures: processing, properties and applications*. Oxford: Elsevier, 2006. 589 p.
40. T. Nakada, M. Mizutani, Y. Hagiwara and A. Kunioka. High-efficiency Cu(In,Ga)Se<sub>2</sub> thin-film solar cells with a CBD-ZnS buffer layer. – *Solar Energy Materials and Solar Cells*, 2001, 67, p. 255–260.
41. C.Falcony, M.Garcia, A. Ortiz and J. C. Alonso. Luminescent properties of ZnS:Mn films deposited by spray pyrolysis. – *Journal of Applied Physics*, 1992, 72, p. 1525–1527.
42. I. P. O'Hare, K. Govender, P. O'Brien and D. Smyth-Boyle. Chemical bath deposition of zinc sulfide from acidic solutions. – *Materials Research Society Symposium Proceedings 668*: Warrendale, PA, 2001, p. H 8.15.1–H.8.15.6.
43. R. Ortega-Borges and D. Lincot. Mechanism of chemical bath deposition of cadmium sulfide thin films in the ammonia-thiourea system. – *Journal of Electrochemical Society*, 1993, 140, p. 3464–3473.
44. T. E. Varitimos and R. W. Tustison. Ion beam sputtering of ZnS thin films. – *Thin Solid Films*, 1987, 151, p. 27–33.

45. J. M. Blackmore and A. G. Cullis. The structure of ZnS thin films deposited by r.f. sputtering. – *Thin Solid Films*, 1991, 199, p. 321–334.
46. L.–X. Shao, K.–H. Chang and H.–L. Hwang. Zinc sulfide thin films deposited by RF reactive sputtering for photovoltaic applications. – *Applied Surface Science*, 2003, 212–213, p. 305–310.
47. M. Oikkonen, M. Blomberg, T. Tuomi and M. Tammenmaa. X-ray diffraction study of microstructure in ZnS thin films grown from zinc acetate by atomic layer epitaxy. – *Thin Solid Films*, 1985, 124, p. 317–321.
48. B. W. Sanders and A. Kitai. Zinc oxysulfide thin films grown by atomic layer deposition. – *Chemistry of Materials*, 1992, 4, p. 1005–1011.
49. T. Suntola and J. Hyvärinen. Atomic Layer Deposition. – *Annual Review Materials Science*, 1985, 15, p. 177–195.
50. Y. S. Kim and S. J. Yun. Studies on polycrystalline ZnS thin films grown by atomic layer deposition for electroluminescent applications. – *Applied Surface Science*, 2004, 229, p. 105–111.
51. N. H. Tran, R. N. Lamb and G. L. Mar. Single source chemical vapour deposition of zinc sulphide thin films film composition and structure. – *Colloids and Surfaces A*, 1999, 155, p. 93–100.
52. F. Zhenyi, C. Yichao, H. Yongliang, Y. Yaoyuan, D. Yanping, Y. Zewu, T. Hongchang, X. Hongtao and W. Heming. CVD growth of bulk polycrystalline ZnS and its optical properties. – *Journal of Crystal Growth*, 2002, 237–239, p. 1707–1710.
53. E. Y. M. Lee, N. H. Tran, J. J. Russell and R. N. Lamb. Structure evolution in chemical vapor-deposited ZnS films. – *Journal of Physical Chemistry B*, 2003, 107, p. 5208–5211.
54. K. Yamaguchi, T. Yoshida, D. Lincot and H. Minoura. Mechanistic study of chemical deposition of ZnS thin films from aqueous solutions containing zinc acetate and thioacetamide by comparison with homogeneous precipitation. – *Journal of Physical Chemistry B*, 2003, 107, p. 387–397.
55. T. B. Nasr, N. Kamoun, M. Kanzari and R. Bennaceur. Effect of pH on the properties of ZnS thin films grown by chemical bath deposition. – *Thin Solid Films*, 2006, 500, p. 4–8.
56. J. Vidal, O. Vigil, O. Melo, N. Lopez and O. Zelaya–Angel. Influence of NH<sub>3</sub> concentration and annealing in the properties of chemical bath deposited ZnS films. – *Materials Chemistry and Physics*, 1999, 61, p. 139–142.
57. A. Antony, K. V. Murali, R. Manoy and M. K. Jayaraj. The effect of the pH value on the growth and properties of chemical–bath–deposited ZnS thin films. – *Materials Chemistry and Physics*, 2005, 90, p. 106–110.
58. X.D. Gao, X.M. Li and W.D. Yu. Morphology and optical properties of amorphous ZnS films deposited by ultrasonic–assisted successive ionic layer adsorption and reaction method. – *Thin Solid Films*, 2004, 468, p. 43–47.

59. S. Lindroos, Y. Charreire, D. Bonnin and M. Leskelä. Growth and characterization of zinc sulfide thin films deposited by the successive ionic layer adsorption and reaction (SILAR) method using complexed zinc ions as the cation precursor. – *Materials Research Bulletin*, 1998, 33, p. 453–460.
60. B. Su and K. L. Choy. Electrostatic assisted aerosol jet deposition of CdS, CdSe and ZnS Thin Films. – *Thin Solid Films*, 2000, 361, p. 102–106.
61. F.J. Martin, H. Albers, P.V. Lambeck, G.M.H. Velde and Th.J.A. Popma. Luminescent thin films by the chemical aerosol deposition technology. – *Journal of Aerosol Science*, 1991, 22, p. S435–438.
62. N. Tonhe, S. Tamaki and K. Okuyama. Formation of Fine Particles of Zinc Sulphide from thiourea complexes by spray pyrolysis. – *Japanese Journal of Applied Physics*, 1995, 34, p. L207–L209.
63. P. Bombicz, J. Madarasz, M. Krunks, L. Niinistö and G. Pokol. Multiple secondary interaction arrangement in the crystal structure of dichlorobis(thiourea-S)-zinc(II). – *Journal of Coordination Chemistry*, 2007, 60, p. 457–464.
64. J. Madarasz, M. Krunks, L. Niinistö and G. Pokol. Evolved gas analysis of Dichlorobis(thiourea)Zinc(II) by coupled TG-FTIR and TG/DTA-MS techniques. – *Journal of Thermal Analysis and Calorimetry*, 2004, 78, p. 679–686.
65. G.-C. Yi, C. Wang and W. II Park. ZnO nanorods: synthesis, characterization and applications. – *Semiconductors Science and Technology*, 2005, 20, p. S22–S34.
66. Ü. Özgür, Y. I. Alivov, C. Liu, A. Teke, M. A. Reshchikov, S. Dogan, V. Avrutin, S.-J. Cho, and H. Morkoç. A comprehensive review of ZnO materials and devices. – *Journal of Applied Physics*, 2005, 98, p. 041301-1–041301-103.
67. Z. L. Wang. Zinc oxide nanostructures: growth, properties and applications. – *Journal of Physics: Condensed Matter*, 2004, 16, p. R829–R858.
68. R.W. Whatmore. Pyroelectric devices and materials. – *Reports on Progress in Physics*, 1986, 49, p. 1335–1386.
69. T. Steiner. Semiconductor nanostructures for optoelectronic applications. – Norwood: Artech Publisher House, 2004. 412 p.
70. M. H. Huang, S. Mao, H. Feick, H. Yan, Y. Wu, H. Kind, E. Weber, R. Russo and P. Yang. Room-temperature ultraviolet nanowire nanolasers. – *Science*, 2001, 292, p. 1897-1899.
71. C. S. Rout, S. H. Krishna, S.R.C. Vivekchand, A. Govindaraj and C.N.R. Rao. Hydrogen and ethanol sensors based on ZnO nanorods, nanowires and nanotubes. - *Chemical Physics Letters*, 2006, 418, p. 586–590.
72. Y. Lv, L. Guo, H. Xu and X. Chu. Gas-sensing properties of well-crystalline ZnO nanorods grown by a simple route. – *Physica E*, 2007, 36, p. 102–105.

73. A. K. Wanekaya, W. Chen, N. V. Myung and A. Mulchandani. Nanowire-based electrochemical biosensor. – *Electroanalysis*, 2006, 18, p. 533–550.
74. X. Jiaqiang, C. Yuping, C. Daoyong and S. Jianian. Hydrothermal synthesis and gas sensing characters of ZnO nanorods. – *Sensors and Actuators B*, 2006, 113, p. 526–531.
75. C. Wang, X. Chu and M. Wu. Detection of H<sub>2</sub>S down to ppb levels at room temperature using sensors based on ZnO nanorods. – *Sensors and Actuators B*, 2006, 113, p. 320–323.
76. T T Chen, C L Cheng, S-P Fu and Y F Chen. Photoelastic effect in ZnO nanorods. – *Nanotechnology*, 2007, 18, p. 225705-225709.
77. J. B. Baxter and E. S. Aydil. Nanowire-based dye-sensitized solar cells. – *Applied Physics Letters*, 2005, 86, p. 053114–053117
78. M. Law, L. E. Greene, J. C. Johnson, R. Saykally, and P. Yang. Nanowire dye-sensitized solar cells. – *Nature Materials*, 2005, 4, p. 455-459.
79. P. Charoensirithavorn and S. Yoshikawa. High-efficiency dye-sensitized solar cell based on ZnO nanorod arrays electrode. - *Materials Research Society Symposium Proceedings 974*: 2007, p. 0974-CC07-10
80. A. Fujishima, and K. Honda. Electrochemical photolysis of water at a semiconductor electrode. – *Nature*, 1972, 238, p. 37–38.
81. R. Tena-Zaera, M. A. Ryan, A. Katty, G. Hodes, S. Bastide and C. Lévy-Clément. Fabrication and characterization of ZnO nanowires/CdSe/CuSCN eta-solar cell. – *Comptes Rendus Chimie*, 2006, 9, p. 717–729.
82. L. Bahadur, M. Hamdini, J. F. Koeing, and. P. Chartier. Studies on semiconducting thin films prepared by the spray pyrolysis technique for photoelectrochemical solar cell applications: Preparation and properties of ZnO. - *Solar Energy Materials*, 1986, 14, p.107-120.
83. S. P. S. Arya, A. D'Amico and E. Verona. Study of sputtered ZnO-Pd thin films as solid state H<sub>2</sub> and NH<sub>3</sub> gas sensors. - *Thin Solid Films*, 1988, 157, p. 169-174.
84. A: Ortiz, M. Garcia, C. Falcony. Photoluminescent properties of indium-doped zinc oxide films prepared by spray. – *Thin Solid Films*, 1992, 207, p. 175-180.
85. F. Paraguay D., W. Estrada L., D.R. Acosta N., E. Andrade and M. Miki-Yoshida. Growth, structure and optical characterization of high quality ZnO thin films obtained by spray pyrolysis. – *Thin Solid Films*, 1999, 350, p. 192-202.
86. R. Ayouchi, D. Leinen, F. Martin, M. Gabas, E. Dalchiele and J.R. Ramos-Barrado. Preparation and characterization of transparent ZnO thin films obtained by spray pyrolysis. – *Thin Solid Films*, 2003, 426, p. 68-77.
87. B.J. Lokhande, P.S. Patil and M.D. Uplane. Deposition of highly oriented ZnO films by spray pyrolysis and their structural, optical and electrical characterization. – *Materials Letters*, 2002, 57, p. 573-579.
88. M. Krunko and E. Melikov. Zinc oxide thin films by the spray pyrolysis method. – *Thin Solid Films*, 1995, 270, p. 33-36.



89. M. Quintana, E. Ricra, J. Rodríguez and W. Estrada. Spray pyrolysis deposited zinc oxide films for photo-electrocatalytic degradation of methyl orange: influence of the pH. – *Catalysis Today*, 2002, 76, p. 141–148.
90. K. Belghit, M. A. Subhan, U. Rülhe, S. Duchemin and J. Bougnot. Sprayed ZnO thin films as optical window in CuInSe<sub>2</sub> based solar cells. – *Proceeding 10th European Photovoltaic Solar Energy Conference: 1991*, p. 613-615.
91. A. Smith and R. Rodriguez-Clemente, Morphological differences in ZnO films deposited by the pyrosol technique: effect of HCl. – *Thin Solid Films*, 1999, 345, p. 192-196.
92. A. El Hichou, M. Addou, J. Ebothe, M. Troyon. Influence of deposition temperature (Ts), air flow rate (f) and precursors on cathodoluminescence properties of ZnO thin films prepared by spray pyrolysis. – *Journal of Luminescence*, 2005, 113, p. 183–190.
93. A. R. Abramson, W. Kim, S. T. Huxtable, H. Yan, Y. Wu, R. Fan, A. Majumdar, C. L. Tien and P. Yang. Fabrication and characterization of a nanowire/polymer-based nanocomposite for a prototype thermoelectric device. - *Journal of Microelectromechanical Systems*, 2004, 13, p. 505-513.
94. X. Wang. Large-scale patterned oxide nanostructures: fabrication, characterization and applications. – Ph.D. Thesis, 2005, Georgia Institute of Technology, USA.
95. Y.W. Wang, L.D. Zhang, G.Z. Wang, X.S. Peng, Z.Q. Chu and C.H. Liang. Catalytic growth of semiconducting zinc oxide nanowires and their photoluminescence properties. – *Journal of Crystal Growth*, 2002, 234, p. 171–175.
96. S. Y. Li, C. Y. Lee and T. Y. Tseng. Copper-catalyzed ZnO nanowires on silicon (100) grown by vapor–liquid–solid process. – *Journal of Crystal Growth*, 2003, 247, p. 357–362.
97. J. Grabowska, K.K. Nanda, E. McGlynn, J.-P. Mosnier and M.O. Henry. Studying the growth conditions, the alignment and structure of ZnO nanorods. - *Surface and Coatings Technology*, 2005, 200, p. 1093 – 1096.
98. X. Liu, X. Wu, H. Cao, and R. P. H. Chang. Growth mechanism and properties of ZnO nanorods synthesized by plasma-enhanced chemical vapor deposition. – *Journal of Applied Physics*, 2004, 95, p. 3141–3147.
99. M. Law, J. Goldberger and P. Yang. Semiconductor nanowires and nanotubes. – *Annual Review on Materials Research*, 2004, 34, p.83–122.
100. H. O. Pierson. *H.O. Handbook of Chemical Vapor Deposition - Principles, Technology and Applications (2nd Edition)*. York: William Andrew Publishing, 1999. 500 p.
101. T.Pauporté and D.Lincot. Heteroepitaxial electrodeposition of zinc oxide films on gallium nitride. – *Applied Physics Letters*, 1999, 75, p. 3817–3819.

102. T. Pauporté, D. Lincot, B. Viana and F. Pellé. Toward laser emission of epitaxial nanorod arrays of ZnO grown by electrodeposition. – *Applied Physics Letters*, 2006, 89, p. 233112–233115.
103. S. P. Anthony, J. I. Lee and J. K. Kim. Tuning optical band gap of vertically aligned ZnO nanowire arrays grown by homoepitaxial electrodeposition. – *Applied Physics Letters*, 2007, 90, p. 103107–103110.
104. D. Lincot. Electrodeposition of semiconductors. – *Thin Solid Films*, 2005, 487, p. 40-48.
105. C. Badre, T. Pauporté, M. Turmine and D. Lincot. Tailoring the wetting behavior of zinc oxide films by using alkylsilane self-assembled monolayers. - *Superlattices and Microstructures*, 2007, 42, p. 99–102.
106. J. Elias, R. Tena-Zaera and C. Lévy-Clément. Electrodeposition of ZnO nanowires with controlled dimensions for photovoltaic applications: Role of buffer layer. – *Thin Solid Films*, 2007, 515, p. 8553–8557.
107. X. M. Sun, X. Chen, Z. X. Deng and Y. D. Li. A CTAB-assisted hydrothermal orientation growth of ZnO nanorods. – *Materials Chemistry and Physics*, 2003, 78, p. 99–104.
108. K. Sue, K. Kimura, M. Yamamoto and K. Arai. Rapid hydrothermal synthesis of ZnO nanorods without organics. – *Materials Letters*, 2004, 58, p. 3350–3352.
109. H. Wei, Y. Wu, N. Lun and C. Hu. Hydrothermal synthesis and characterization of ZnO nanorods. – *Materials Science and Engineering A*, 2005, 393, p. 80–82.
110. L. Wu, Y. Wu and W. Lü. Preparation of ZnO Nanorods and optical characterizations. – *Physica E: Low-dimensional Systems and Nanostructures*, 2005, 28, p. 76–82.
111. M. Guo, P. Diao and S. Cai. Hydrothermal growth of well-aligned ZnO nanorod arrays: Dependence of morphology and alignment ordering upon preparing conditions. – *Journal of Solid State Chemistry*, 2005, 178, p. 1864–1873.
112. K. Fukutani, T. Motoi and T. Den. Template-assisted growth of nanowires using novel nanoporous films fabricated by inorganic nano phase separation. - *Materials Research Society Symposium Proceedings 818: Warrendale, PA*, 2004, p. M11.25.1- M11.25.6.
113. K. S. Shankar and A.K. Raychaudhuri. Fabrication of nanowires of multicomponent oxides: Review of recent advances. - *Materials Science and Engineering C*, 2005, 25, p. 738-751.
114. G.S. Wu, T. Xie, X.Y. Yuan, Y. Li, L. Yang, Y.H. Xiao and L.D. Zhang. Controlled synthesis of ZnO nanowires or nanotubes via sol–gel template process. - *Solid State Communications*, 2005, 134, p. 485-489.
115. M. H. Huang, Y. Wu, H. Feick, N. Tran, E. Weber and P. Yang. Catalytic growth of zinc oxide nanowires by vapor transport. – *Advanced Materials*, 2001, 13, p. 113-116.

116. Y. Li, G.W. Meng, L.D. Zhang and F. Phillipp, Ordered semiconductor ZnO nanowire arrays and their photoluminescence properties. - *Applied Physics Letters*, 2000, 76, p. 2011-2013.
117. W. L. Hughes. William L. Synthesis and characterization of zinc oxide nanostructures for piezoelectric applications.– Ph.D. Thesis, 2006, Georgia Institute of Technology, USA.
118. S.-C. Liu and J.-J. Wu. Low-temperature and catalyst-free synthesis of well-aligned ZnO nanorods on Si (100). – *Journal of Materials Chemistry*, 2002, 12, p. 3125–3129.
119. M.C. López, J.P. Espinos, F. Martín, D. Leinen and J.R. Ramos-Barrado. Growth of ZnS thin films obtained by chemical spray pyrolysis: The influence of precursors. - *Journal of Crystal Growth*, 2005, 285, p. 66-75.
120. Spectroscopic tool's web-site, <http://www.chem.uni-potsdam.de/tools/index.html>. Date 14.08.2007.
121. T. Ben Nasrallah, M. Amlouk , J. C. Bernède and S. Belgacem. Structure and morphology of sprayed ZnS thin films. - *Physica Status Solidi (a)*, 2004, 201, p. 3070 – 3076.
122. J.Y. Park, I.O. Jung, J.H. Moon, B.-T. Lee, S.S. Kim, Temperature-induced morphological changes of ZnO grown by MOCVD. – *Journal of Crystal Growth* 2005, 282, p. 353-358.
123. S. Y. Li, P. Lin, C. Y. Lee and T. Y. Tseng. Field emission and photofluorescent characteristics of zinc oxide nanowires synthesized by a metal catalyzed vapor-liquid-solid process. – *Journal of Applied Physics*, 2004, 95, p. 3711-3716.
124. X. Liu, X. Wu, H. Cao and R. P. H. Chang. Growth mechanism and properties of ZnO nanorods synthesized by plasma-enhanced chemical vapor deposition. – *Journal of Applied Physics*, 2004, 95, p. 3141-3147.
125. Ke Yu, Y. Zhang, R. Xu, S. Ouyang, D. Li, L. Luo, Z. Zhu, J. Ma, S. Xie, S. Han and H. Geng. Efficient field emission from tetrapod-like zinc oxide nanoneedles. – *Materials Letters*, 2005, 59, p. 1866–1870.
126. M. Guo, P. Diao, X. Wang and S. Cai. The effect of hydrothermal growth temperature on preparation and photoelectrochemical performance of ZnO nanorod array films. – *Journal of Solid State Chemistry*, 2005, 178, p. 3210–3215.
127. M. Guo, P. Diao and S. Cai, Hydrothermal growth of perpendicularly oriented ZnO nanorod array film and its photoelectrochemical properties. – *Applied Surface Science*, 2005, 249, p. 71–75.
128. R.B.M. Cross, M.M. De Souza and E.M. S. Narayanan. A low temperature combination method for the production of ZnO nanowires. – *Nanotechnology*, 2005, 16, p. 2188–2192.

129. T.-L. Chou and J.-M. Ting. Deposition and characterization of a novel integrated ZnO nanorods/thin film structure. – *Thin Solid Films*, 2006, 494, p.291–295.
130. J. Zhao, Z.-G. Jin, T.Li and X.-X.Liu. Nucleation and growth of ZnO nanorods on the ZnO-coated seed surface by solution chemical method. – *Journal of European Ceramic Society*, 2006, 26, p.2769–2775.
131. B. H. Kong and H. K. Cho. Formation of vertically aligned ZnO nanorods on ZnO templates with the preferred orientation through thermal evaporation. – *Journal of Crystal Growth*, 2006, 289, p. 370–375.
132. T. Schilling and D. Frenkel. Self-poisoning of crystal nuclei in hard-rod liquids. – *Journal of Physics: Condensed Matter*, 2004, 16, p. S2029-S2036.
133. Z. Zhu, T. Andelman, M. Yin, T.-L. Chen, S.N. Ehrlich, S.P.O'Brien and R.M. Osgood. Synchrotron X-ray scattering of ZnO nanorods: Periodic ordering and lattice size. – *Journal of Materials Research*, 2005, 20, p. 1033-1041.
134. A. Sugunan, H.C. Warad, M. Boman and J. Dutta. Zinc oxide nanowires in chemical bath on seeded substrates: Role of hexamine. – *Journal of Sol–Gel Science and Technology*, 2006, 39, p. 49-56.
135. D.Y. Lee, C.H. Choi and S.H. Kim. Growth and characterization of ZnO film on Si(111) substrate by helicon wave plasma-assisted evaporation. – *Journal of Crystal Growth*, 2004, 268, p. 184-191.
136. L. Wu, Y. Wu, X. Pan and F. Kong. Synthesis of ZnO nanorod and the annealing effect on its photoluminescence property. – *Optical Materials*, 2006, 28, p. 418-422.
137. K.A. Alim, V.A. Fonoberov, M. Shamsa and A. Baladin. Micro-Raman investigation of optical phonons in ZnO nanocrystals. – *Journal of Applied Physics*, 2005, 97, p. 124313-124318.
138. V.Gupta, P. Bhattacharya, Y.I. Yusuk, K. Sreenivas and R.S. Katiyar. Optical phonon modes in ZnO nanorods on Si prepared by pulsed laser deposition. – *Journal of Crystal Growth*, 2006, 287, p. 39-43.
139. D.-F. Zhang, L.-D. Sun and C.H. Yan. Chem. Optical properties of ZnO nanoplatelets and rectangular cross-sectioned nanowires. – *Physical Letters*, 2006, 422, p. 46-50.
140. H.-C. Hsu, H.-M. Cheng, C.-Y.Wu., H.-S. Huang, Y.-C. Lee and W.-F. Hsieh. Luminescence of selective area growth of epitaxial ZnO nanowires and random-growth-oriented nanobelts. – *Nanotechnology*, 2006, 17, p. 1404–1407.

## **Appendix A**

### **Article I**

**T. Dedova**, M. Krunks, O. Volobujeva and I. Oja. ZnS thin films deposited by spray pyrolysis technique. - *Physica Status Solidi c*, 2005, 3, p.1161-1166.

## **Appendix A**

### **Article II**

**T. Dedova**, A. Mere, O. Kijatkina, I. Oja, O. Volobujeva and M. Krunks.  
Structural and optical characterization of sprayed ZnS thin films. - Proceedings of  
SPIE 5946: 2005, p.34-40.

## **Appendix A**

### **Article III**

M. Krunk, **T. Dedova** and I. Oja. Spray pyrolysis deposition of nanostructured Zinc Oxide thin films. - Thin Solid Films, 2006, 515, p. 1157-1160.

## **Appendix A**

### **Article IV**

**T. Dedova, M. Krunks, M. Grossberg, O. Volobujeva and I. Oja Acik. A novel deposition method to grow ZnO nanorods: spray pyrolysis. - Superlattices and Microstructures, 2007, 42, p. 444-450.**



## **Appendix A**

### **Article V**

**T. Dedova**, M. Krunks, A. Mere, J. Klauson and O. Volobujeva. Preparation of shape and size-controlled zinc oxide nanostructures by chemical spray pyrolysis technique. Materials Research Society Symposium Proceedings 957: Warrendale, PA, 2007, p. 0957-K10-26.

## **Appendix A**

### **Article VI**

**T. Dedova**, O. Volobujeva, J. Klauson, A. Mere and M. Krunks. ZnO nanorods via spray deposition of solutions containing zinc chloride and thiocarbamide. - *Nanoscale Research Letters, Nanoexpress*, 2007, 2, p.391-396.

## **Appendix A**

### **Patent application VII**

M. Krunk, I. Oja and **T. Dedova**. Method of preparing zinc oxide nanorods on a substrate by chemical spray pyrolysis, international patent application WO2006/108425 (Priority No. US20050671232P, priority date 04/14/2005).

**Appendix B**

Curriculum Vitae

## Appendix B

### Curriculum Vitae

|                       |  |
|-----------------------|--|
| Ees- ja perekonnanimi | Tatjana Dedova   |
| Sünniaeg ja –koht     | 19.10.1978 Eesti   |
| E-post                | <a href="mailto:dedova@staff.ttu.ee">dedova@staff.ttu.ee</a>   |
| Hariduskäik           | 2003-2007 Tallinna Tehnikaülikool, Keemia- ja materjalitehnoloogia teaduskond, doktorantuur<br>2003- Tallinna Tehnikaülikool, Keemia- ja materjalitehnoloogia teaduskond, loodusteaduste magistrikraad<br>2001- Tallinna Tehnikaülikool, Keemia- ja materjalitehnoloogia teaduskond, loodusteaduste bakalaureusekraad  |
| Teenistuskäik         | 1997- Pähklimäe Gümnaasium, keskharidus<br>2003- Tallinna Tehnikaülikool, Materjaliteaduse instituut, teadur<br>2001-2003- Tallinna Tehnikaülikool, Materjaliteaduse instituut, insener  |
| Kaitstud lõputööd     | „CdS sadestamine ja selle eeltötluse mõju päikeseelementide väljudparameetritele” magistritöö, juhendaja vanemteadur Mare Altosaar<br>„Raskmetallide järjestikekstraktsioon turbast”, bakalaureusetöö, juhendaja Prof. Ivars Neretnieks (KTH, Rootsi), Prof. Rein Munter (TTÜ)   |
| Täiendõpe             | aug. 21-25, 2006, „Young scientist summer school on photovoltaics”, Villa Andropoff, Pärnumaa, Eesti<br>oct.- nov., 2005, Research Centre of Netherlands (ECN), Petten, Holland, guest researcher<br>aug. 27–sept. 4, 2005, 1st International Summer Academy on Photovoltaics, Berliin, Saksamaa<br>aug. 27-31. , 2004, 6-th International Conference-School, „Advanced Materials and Technologies“, Palanga, Leedu<br>sept. 14-19 Summerschool Quantsol 2003, „Basic principles and new concepts in quantum solar energy conversion, Hirshegg, Austria<br>mai. 27-jun.3, 2002 „Thin Film Deposition and |

Applications“, Uppsala, Rootsi  
2001 (Jan.-Jun.) Kuninglik Tehnoloogia Instituut,  
KTH, Stockholm, vahetustudeng

## Appendix B

### Curriculum Vitae

|                         |   |
|-------------------------|---|
| First name and surname  | Tatjana Dedova  |
| Date and place of birth | 19.10.1978 Estonia  |
| E-mail                  | <a href="mailto:dedova@staff.ttu.ee">dedova@staff.ttu.ee</a>  |
| Education               | 2003-2007 Tallinn University of Technology, Faculty of Chemical and Materials Technology, doctoral study<br>2003- Tallinn University of Technology, Faculty of Chemical and Materials Technology, Master of Science in Natural Sciences<br>2001- Tallinn University of Technology, Faculty of Chemical and Materials Technology, Bachelor of Science in Natural Sciences<br>1997- Narva Pähklikimäe Gymnasium |
| Professional experience | 2003- up to now Tallinn University of Technology, Department of Materials Science, researcher<br>2001- 2003 Tallinn University of Technology, Department of Materials Science, engineer   |
| Defended dissertations  | „Influence of chemically deposited CdS and absorber surface pretreatment on solar cell's output parameters”, master thesis, supervisor senior research scientist Mare Altosaar<br>“Sequential extraction of heavy metals from peat“, bachelor thesis, supervisor Prof. Ivars Neretnieks (KTH, Sweden), Prof. Rein Munter (TTÜ)  |
| Training courses        | Aug. 21-25, 2006, „Young scientist summer school on photovoltaics”, Villa Andropoff, Pärnumaa, Estonia<br>Oct.- Nov., 2005, Research Centre of Netherlands (ECN), Petten, Holland, guest researcher<br>Aug. 27–Sept. 4, 2005, 1st International Summer Academy on Photovoltaics, Berliin, Saksamaa<br>Aug. 27-31., 2004, 6-th International Conference-School, „Advanced Materials and Technologies“,         |

Palanga, Leedu  
Sept. 14-19, 2003, Summerschool Quantsol,  
„Basic principles and new concepts in quantum  
solar energy conversion, Hirshegg, Austria  
Mai. 27-Jun.3, 2002, „Thin Film Deposition and  
Applications“, Uppsala, Rootsi  
Jan.-Jun., 2001, Royal Institute of Technology,  
KTH, Stockholm, exchange student

### List of publications

1. **T. Dedova**, O. Volobujeva, J. Klauson, A. Mere, M. Krunks, ZnO nanorods via spray deposition of solutions containing zinc chloride and thiocarbamide, *Nanoscale Research Letters*, Nanoexpress, 2 (8), 2007, pp. 391-396
2. **T. Dedova**, M. Krunks, A. Mere, J. Klauson, O. Volobujeva, Preparation of shape and size-controlled zinc oxide nanostructures by chemical spray pyrolysis technique, in *Zinc Oxide and Related Materials*, edited by J. Christen, C. Jagadish, D.C. Look, T. Yao, F. Bertram (Mater. Res. Soc. Symp. Proc. **957**, Warrendale, PA, 2007), 0957-K10-26
3. **T. Dedova**, M. Krunks, M. Grossberg, O. Volobujeva, I. Oja Acik, A novel deposition method to grow ZnO nanorods: spray pyrolysis, *Superlattices and Microstructures*, 42, (2007), pp. 444-450
4. **T. Dedova**, J. A. Wienke, M. J. A. A. Goris, M. Krunks, Characterization of the chemical bath deposited In(OH)<sub>x</sub>Sy films: Importance of the growth conditions, *Thin Solid Films*, 515, (2007), pp. 6064-6067
5. M. Krunks, **T. Dedova**, I. Oja, Spray pyrolysis deposition of nanostructured Zinc Oxide thin films, *Thin Solid Films*, 515, (2006), pp. 1157-1160
6. J. Hiie, **T. Dedova**, V. Valdna, K. Muska, Comparative study of nanostructured CdS thin films prepared by CBD and spray pyrolysis: Annealing effect, *Thin Solid Films*, 511-512, (2006), pp. 443-447
7. **T. Dedova**, M. Krunks, O. Volobujeva, I. Oja, ZnS thin films deposited by spray pyrolysis technique, *Physica Status Solidi c*, 2, No.3 (2005) pp. 1161-1166.
8. **T. Dedova**, A. Mere, O. Kijatkina, I. Oja, O. Volobujeva, M. Krunks, Structural and optical characterization of sprayed ZnS thin films, in *Proceedings of SPIE*, vol. 5946 "Optical Materials and Applications", edited by Arnold Rosental, (SPIE, 2005) pp.34-40.

### Patent applications:

9. M. Krunks, I. Oja, **T. Dedova**, Method of preparing zinc oxide nanorods on a substrate by chemical spray pyrolysis, international patent application



WO2006/108425, (Priority No. US20050671232P, priority date 04/14/2005.).

10. M. Krunks, A. Katerski, **T. Dedova**, A. Mere, I. Oja Acik, Photovoltaic Cell based on ZnO nanorods, US patent application, (Priority No. US60/948508, priority date 07/09/2007).